Conducting polypyrrole-coated macroporous melamine sponges: a simple toy or an advanced material?

Conducting polypyrrole-coated macroporous melamine sponges: a simple toy or an advanced material?

Jaroslav Stejskal[1]• Irina Sapurina[2,3] • Jarmila Vilčáková[2] • Petr Humpolíček[2] • Thanh Huong Truong[2] • Mikhail A. Shishov[3] • Miroslava Trchová[4] • Dušan Kopecký[4] • Zdeňka Kolská[5] • Jan Prokeš[6] • Ivo Křivka[6]

** Jaroslav Stejskal stejskal@imc.cas.cz*

[1] Institute of Macromolecular Chemistry, Academy of Sciences of the Czech Republic, 162 06 Prague 6, Czech Republic

[2] Centre of Polymer Systems, Tomas Bata University in Zlin, 760 01 Zlin, Czech Republic

[3] Institute of Macromolecular Compounds, Russian Academy of Sciences, St. Petersburg, Russian Federation 199004

[4] University of Chemistry and Technology, Prague, 166 28 Prague 6, Czech Republic

[5] Faculty of Science, J.E. Purkyně University, 400 96 Ústí nad Labem, Czech Republic

[6] Faculty of Mathematics and Physics, Charles University, 180 00 Prague 8, Czech Republic

** Jaroslav Stejskal stejskal@imc.cas.cz*

Abstract

The present feature article offers a concise overview of recent research progress of the authors working in the design of macroporous conducting materials represented by polypyrrole-coated melamine sponges. The article highlights innovative results from the authors and suggests a perspective for future directions in the field of macroporous conducting polymer composites. The article also overviews this particular subject area and defines key challenges for this emerging field. The feasibility of diverse applications of polypyrrole/melamine sponges is demonstrated and includes deformation-sensitive materials, electromagnetic radiation shielding and electrically heated insulation materials. Cytotoxicity is addressed with respect to applications in biomedicine, and the adsorption of an organic dye serves as an example of the uses in environmental water-pollution treatment. A single-step deposition of polypyrrole during the oxidative polymerization of pyrrole provides the uniform coating of the sponge with an organic conducting phase. The conductivity of sponges was of the order of 10^{-3} S cm^{-1}, increased with polypyrrole loading, and also by two orders of magnitude after the compression. Derived materials have also been prepared and tested. They are represented by polypyrrole-coated sponge converted by pyrolysis to a macroporous nitrogen-containing carbon, magnetic ferrosponge obtained by incorporation of magnetite, or the conventional globular polypyrrole coating replaced with polypyrrole nanotubes. Polypyrrole can also be simply decorated with silver nanoparticles. The macroporous conducting polypyrrole/melamine

sponges and derived materials are considered to be of future scientific interest with broad application potential.

Graphic abstract

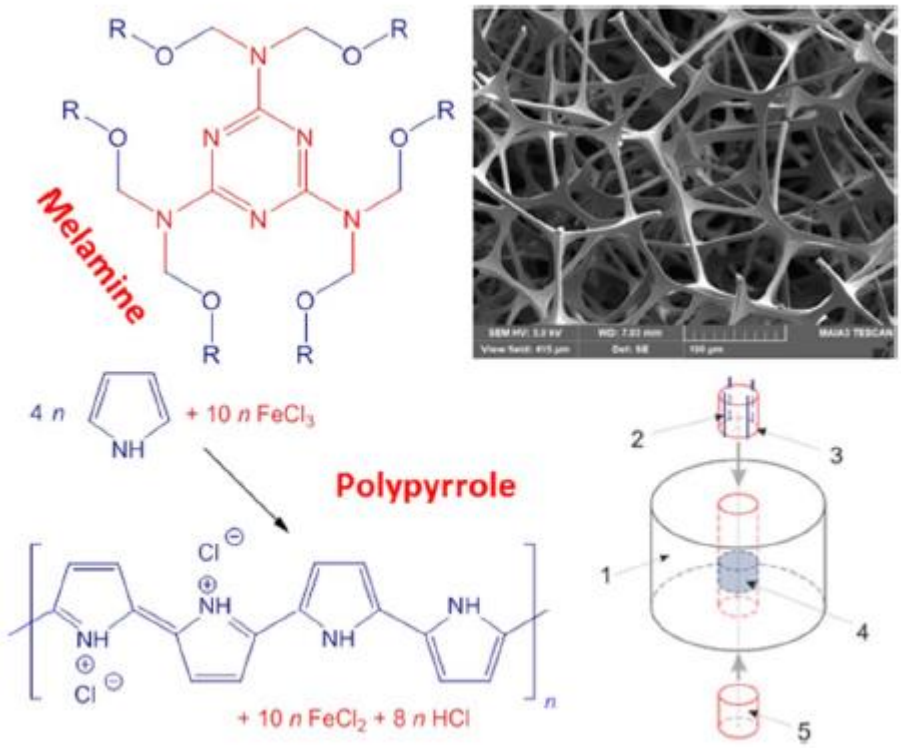

Keywords Conducting polymer ■ Macroporous sponge ■ Melamine ■ Polypyrrole ■ Nitrogen-containing carbon ■ Polypyrrole nanotubes

Preamble

Conducting polymers, such as polyaniline and polypyrrole and their ring-substituted derivatives, have an application potential due to their electronic and ionic conductivity, electroactivity, stimuli responsivity and various physico-chemical properties that include adsorption phenomena, electromagnetic radiation absorption, catalysis, biointeractions, etc. They are simply prepared by the chemical or electrochemical polymerizations of respective monomers and obtained as intractable powders, thin films, hydrogels or colloids. From the processing and application point of view, the strategy based on the coating of various substrates that provide the desired materials properties is widely used. The deposition of conducting polymers in-situ during the chemical polymerization on templates immersed in the aqueous reaction mixture is easy. Particulate inorganic or organic objects of various shapes modified with conducting polymers serve as fillers in the composites, the coating of fibres and textiles provides another suitable application form. Three-dimensional macroporous materials represented by sponges coated with conducting polymers have only recently come to the forefront.

Introduction

The soft three-dimensional composite materials incorporating conducting polymers are demanded especially in the design of electroactive and biocompatible systems suitable for biomedical applications (Stejskal **2017**; Tomczykowa and Polonska-Brzezinska **2019**; Lavrdor et al. **2021**). Open-cell polymer sponges and foams served as templates for the in-situ deposition of conducting polymers (Chen et al. **2017a**; Li et al. **2019**, **2020**a) but the resulting products still suffered from the inhomogeneity with respect to the conducting-phase distribution, due to the concentration gradients of reactants produced within the coated template. In the routine preparation, the sponges have been penetrated with a monomer and transferred to the solution of an oxidant or vice versa. By using such a two-step approach, the applicable conducting materials can be prepared but the distribution of a conducting polymer within the matrix is uneven (Stejskal **2017**) because the conducting polymer is preferentially produced at the interface where reactants meet (Blinova et al. **2007**). The properties of such well-applicable materials are still size- and shape-dependent. Most of reports concern polyurethane sponges that have been proposed for diverse directions including microorganism immobilization (Antonio-Cremona et al. **2015**), pressure or force sensors (Gunasekara et al. **2020**; Wan et al. **2020**), bioanode in fuel cells (Pérez-Rodríguez et al. 2016; Xu et al. **2018**), water-pollutant removal (Vali et al. **2018)** or as a wound-dressing material (dos Santos et al. **2018**). Polydimethylsiloxane sponge coated with polypyrrole was used as a compressible capacitance sensor (Chen et al. **2020a**).

Melamine, or more precisely melamine-formaldehyde, sponges (Feng and Yao **2018**) (**Fig. 1**) have been extensively used as supports in lightweight sound-proofing materials (Yan et al. **2020**) due to its high sound absorption with accompanying excellent thermal insulation performance (Gu et al. **2020**). Due to a high nitrogen content, the flame-retardation properties of melamine foam prevent a fire hazard (Ruan et al. **2014**). Melamine sponges are also advertised as “magic” abrasive cleaners. The deposition of conducting polymers may thus convert the sponge to a functional material with extended applicability.

Melamine sponge has only recently been used as a support for the deposition of conducting polymer, polypyrrole. For example, the sponge penetrated with solid iron(III) chloride as oxidant was exposed to pyrrole vapours and thus coated with polypyrrole. The product was subsequently applied as a material for the rapid and efficient oil-water separation (Chen et al. **2017a**) or as a compressible electrochemical capacitor (Chang et al. **2019)**. In interfacial method, pyrrole solution in cyclohexane was added to melamine sponge swollen with aqueous oxidant solution. Applications concerned solar desalination (Li et al. **2019**) or the design of a flexible supercapacitor (Sun et al. 2019). Polypyrrole was only exceptionally prepared electrochemically on gold-sputtered substrates (Liu et al. **2019**).

The present review is devoted especially to a single-step procedure for the homogeneous coating of soft macroporous materials with conducting polymer represented by melamine sponge and polypyrrole. Polypyrrole is typically prepared by the oxidation of pyrrole with iron (III) chloride in aqueous medium (**Fig. 2**). Instead of traditional swelling of sponges with one reactant solution followed by the transfer to the second reactant solution, the sponges were immersed in a freshly prepared solution of pyrrole and oxidant. This is the fundamental difference that guarantees the oxidation of pyrrole with iron(III) chloride to proceed homogeneously in the whole volume of the sponge and not only on its external surface.

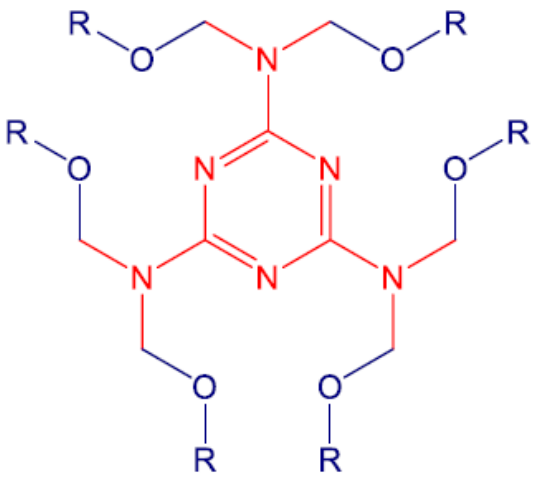

Fig. 1 In melamine sponge, the melamine molecules (red) are linked to formaldehyde units or to other melamine molecules

Coating of melamine sponges with conducting polypyrrole

In the present study, melamine sponge was a commercial product of 100 x 60 x 26 mm^3 size developed by BASF AG (Germany) under the trademark Basotect and distributed as "a magic eraser sponge" by various suppliers, e.g., Drogerie ZDE (Czech Republic). Apparent density of melamine sponge calculated from its mass and geometric dimensions was 8.8 x 10^{-3} g cm^{-3}, the volume fraction of solid melamine phase was 0.63 vol%.

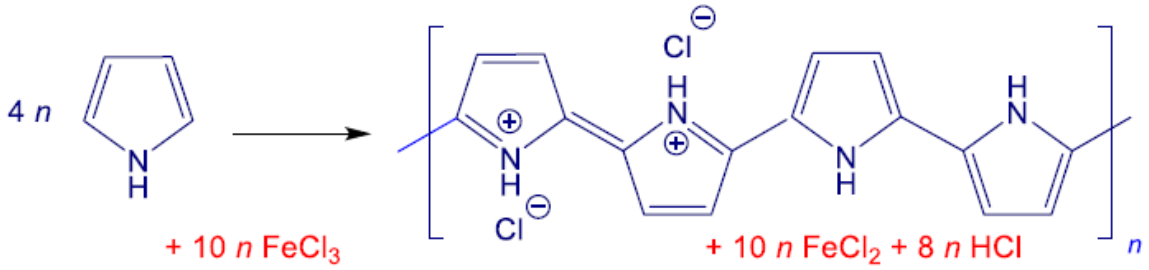

Fig. 2 Pyrrole is oxidized in aqueous medium with iron(III) chloride to polypyrrole hydrochloride. Iron(II) chloride and hydrochloric acid are byproducts

For the coating with polypyrrole (Kopecká et al. **2014**; Stejskal et al. **2016**), the sponges were immersed without any pre-treatment in a freshly prepared aqueous mixture containing 0.2 M pyrrole and 0.5 M iron(III) chloride hex-ahydrate (both from Sigma Aldrich) **(Table 1**). In practice, 14 mL of pyrrole and 135 g of iron(III) chloride hexa-hydrate were separately dissolved in water, and the total volume of both solutions was adjusted to 500 mL. Equal volumes of both solutions were mixed and quickly poured over the sponge. The solutions were pre-cooled to 4 °C in order to slow down the polymerization rate. Air in pores was liberated by squeezing the immersed sponge, i.e. the sponge

became penetrated with the reaction mixture containing both reactants. The polymerization was completed within a few minutes but the sponge was left in the reaction mixture at room temperature for 1 h. The sponge was then removed, suspended repeatedly in excess of 0.2 M hydrochloric acid to remove the residual reactants, byproducts and adhering polypyrrole precipitate generated in aqueous phase outside the sponge. The sponge was repeatedly rinsed with ethanol until no colouration of this solvent was visible and then left to dry in open air.

In other samples, polypyrrole content was reduced by diluting the original 0.2 M concentration of pyrrole to 0.1, 0.05 M, and the samples were denoted as M-1, M-1/2 and M-1/4, respectively, M-0 being the code for uncoated sponge (**Table 1**). The oxidant to monomer mole ratio was maintained at stoichiometric value 2.5 **(Fig. 2**). The polypyrrole content in dry sponge was evaluated from the difference in mass before and after the deposition of polypyrrole (**Table 1**). The coating with polypyrrole manifests itself in change of colour from white to black (**Fig. 3**).

Table 1 Concentration of pyrrole used in the synthesis, the polypyrrole content, *w*, specific surface area, S, pore volume, V, conductivities, σ, at minimum and maximum compression, and a compressibility parameter, Γ, of polypyrrole-coated melamine sponges

Sponge	Pyrrole,[a] mol L^{-1}	*w*, wt%	*S*, m^2g^{-1}	*V*, cm^3g^{-1}	σ_{min},[b] S cm^{-1}	σ_{max},[c] S cm^{-1}	Γ [d]
M-0	0	0	38.8	0.071	–	–	0.467
M-1/4	0.05	21.1	75.2	0.081	9.4×10^{-3}	0.91	0.512
M-1/2	0.1	40.2	51.0	0.022	4.3×10^{-3}	0.21	0.450
M-1	0.2	67.2	30.4	0.017	5.7×10^{-4}	0.062	0.352

[a]Mole ratio [FeCl3]/[Pyrrole] = 2.5. [b]At minimum compression. [c]At maximum compression. [d] Γ = — d[log(dM0)]/d(log p) (cf. the section on compressibility)

Fig. 3 White melamine sponge (M-0; left) becomes black after coating with polypyrrole (M-1; right)

Characterization methods

A Tescan MAIA3 ultra-high-resolution scanning electron microscope was used to characterize the morphology. Thermogravimetric analysis was carried out in air or inert nitrogen atmosphere at 50 mL min^{-1} gas flow and heating rate 10 °C min^{-1} using Perkin Elmer Pyris 1 Thermogravimetric Analyzer.

ATR FTIR spectra were recorded using a Thermo Nicolet NEXUS 870 FTIR spectrometer (Thermo Scientific, Madison, WI, USA) in a dry air-purged environment with mercury cadmium telluride detector in the wavelength range from 400 to 4000 cm^{-1}. MKII Golden Gate™ Heated Diamond ATR Top-Plate single reflection system (Specac Ltd, Orpington, Great Britain) was applied for the measurements of spectra. Typical parameters used: 256 of sample scans, resolution 4 cm^{-1}, Happ-Genzel apodization, potassium bromide beam-splitter. Raman spectra were collected on a Renishaw inVia Reflex Raman spectrometer (Leica DM LM microscope; objective magnification 50 x) with a near infrared diode 785 nm laser (holographic grating 1200 lines mm^{-1}).

Specific surface area was determined with adsorption and desorption isotherms using a NOVA3200 (Quan-tachrome Instruments). Samples were degassed for 24 h at 100 °C, then isotherms were recorded with nitrogen (Linde, 99.999%). Brunauer-Emmett-Teller (BET) analysis has been applied for the total surface area determination and Barrett-Joyner-Halenda (BJH) model for pores volume. Each sample was measured four times with experimental error of ca 5%.

Cylinders 10 mm in diameter were cut with a circular cork-cutter knife from the sponge and adjusted to ca 8 mm length with gentle pressure. Their conductivity was determined by four-point van der Pauw method in a cylindrical glass cell with inner diameter of 10 mm between an insulating support and a glass piston carrying four platinum/rhodium electrodes on the perimeter of its base. The set-up used the current source Keithley 220, a Keithley 2010 multimeter and a Keithley 705 scanner with a Keithley 7052 matrix card. The pressure applied to the sponge was controlled with a L6E3 load cell (Zemic Europe BV, The Netherlands). The thickness of the sponge during the compression was determined with a displacement meter Digimatic Indicator 543-122FB (Mitutoyo Corp., Japan).

The cytotoxicity was tested according to the ISO 10-993 on extracts prepared at 0.02 g of tested material per 1 mL of cultivation medium. The parent extracts (100%) were then diluted in culture medium to obtain a series of dilutions with concentrations of 100, 75, 50, 25, 10, 5 and 1%. All extracts were used up to 24 h. The mouse embryonic fibroblast cell line (ATCC CRL-1658 NIH/3T3, USA) was used in the test. The cultivation was done according to ATCC protocol. The MTT assay was used to determine the cell viability. The optical absorbance was measured at 570 nm and the reference wavelength was adjusted to 690 nm. The results are presented as reduction of cell viability in percentage when compared with cells cultivated in medium without the extracts of tested materials. Morphology of cells from the culture plates was observed using an inverted Olympus phase contrast microscope (IX 81).

Properties of polypyrrole/melamine sponges

Morphology

Any surface immersed in the reaction mixture containing pyrrole and oxidant becomes coated with a polypyrrole film **(Fig. 3**). The surface polymerization is preferred over the polymerization in the bulk (Fedorova and Stejskal **2002**) that produces a polypyrrole precipitate. Melamine sponge has open-cell structure with the cell size ≈100 pm (**Fig. 4**). The coating of melamine sponge with polypyrrole is clearly visible at higher magnifications and includes some adhering polymer nanoparticles.

Free polypyrrole produced outside melamine has not been detected on micrographs but it is also present inside the sponge. This clearly manifests itself as an emanating aerosol “smoke” composed of released polypyrrole nanoparticles when the sponge is compressed or cut (Stejskal et al. **2021a**). These nanoparticles just leave the macroporous structure and, for that reason, they are not visible by the microscope. Their presence, however, is clearly demonstrated after carbonization (cf. the section on nitrogen-containing carbons). The formation of the accompanying precipitate can be prevented by using a 2 wt% solution of poly(A-vinylpyrrolidone) as a reaction medium instead of water (Stejskal et al. **2021a**). Under such coating conditions, colloidal dispersion nanoparticles are produced in place of a precipitate (Riede et al. **2002**) and they are easily washed out of the sponge.

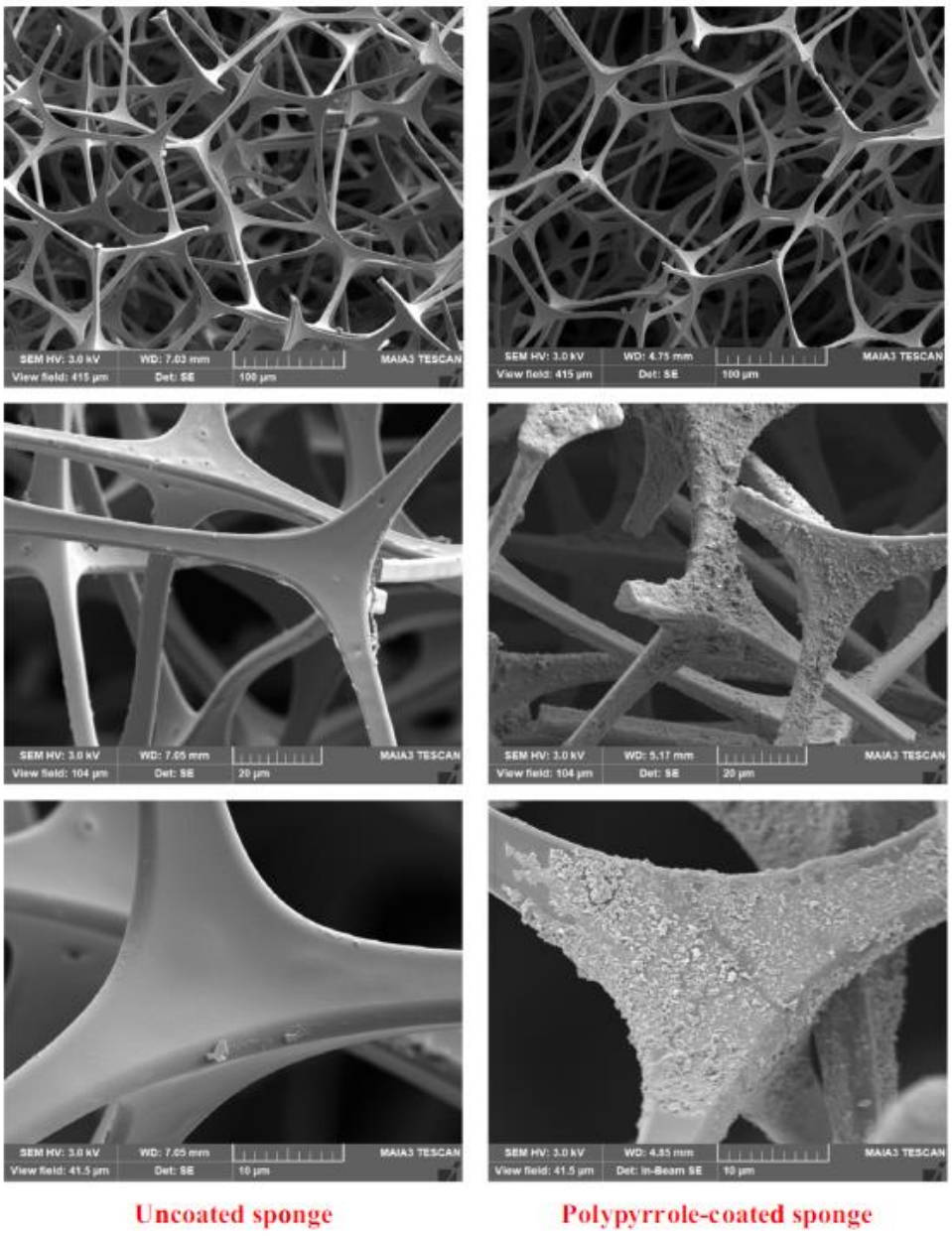

Fig. 4 Melamine sponge before (left) and after coating with the highest amount of polypyrrole (M-1; right): overview (top) and details (bottom). Scale bars 100, 20 and 10 µm

FTIR and Raman spectra

The attenuated total reflectance (ATR) infrared spectra of polypyrrole and polypyrrole-coated sponge are very close each to other **(Fig. 5**), and they correspond to the conducting polypyrrole salt (Stejskal and Trchová **2018**) (**Fig. 2)**. The spectrum of polypyrrole deposited on the sponge is of higher quality due to the better contact with the ATR crystal when recorded by using this surface-sensitive technique. Small shifts of the maxima of the main bands of polypyrrole in its spectrum correspond to the overlapping with the bands observed in the spectrum of neat melamine sponge **(Fig. 5)**. This is connected with the penetration of the infrared radiation through the thin polypyrrole coating.

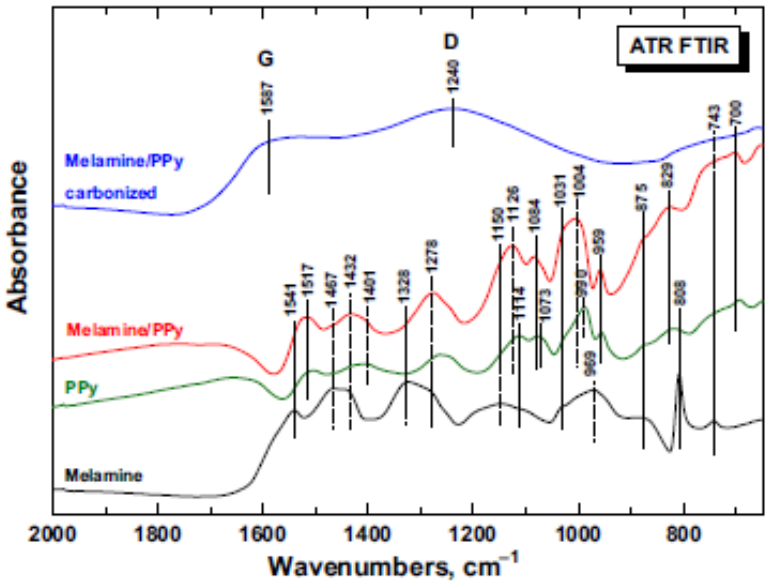

Fig. 5 ATR FTIR spectra of melamine sponge, polypyrrole (PPy) and polypyrrole-coated sponge. The spectrum of polypyrrole-coated sponge carbonized in inert atmosphere at 650 °C is also included (cf. the section on nitrogen-containing carbons)

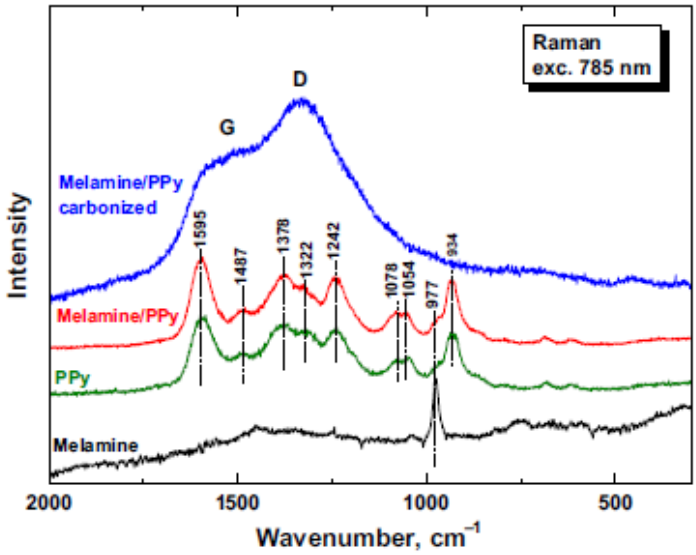

Fig. 6 Raman spectra of melamine sponge, polypyrrole, polypyrrole-coated sponge before and after the carbonization in inert atmosphere at 650 °C

In addition, we observe that Raman spectra of polypyrrole and polypyrrole-coated sponge are practically identical and correspond to the conducting polypyrrole (Peng et al. **2019**) (**Fig. 6**). The energy of laser excitation wavelength 785 nm is in resonance with the energy of delocalized polarons and bipolarons in the structure of the conducting polypyrrole. The penetration depth of the laser beam is therefore small and no spectral features of melamine have been observed in the spectrum. This also means that the coating of melamine threads with polypyrrole is complete.

Thermogravimetric analysis

Thermogravimetric analysis offers an insight into the thermal stability of a composite and its components. Melamine is thermally stable and the first decomposition changes are observed only above 400 °C (**Fig. 7a**). The thermogravimetric curves recorded in air and in inert nitrogen atmosphere are virtually identical up to 700 °C. Melamine is decomposed in air above this limit leaving just a few per cent residue, while in inert atmosphere, the degradation still continues (**Fig. 7b**). It was nevertheless reported that spongelike structure of melamine sponge can be preserved even after the carbonization at 1000 °C (Peng et al. **2019**; Ye et al**. 2019**). This is due to high content of nitrogen in melamine sponge (**Fig. 1**), which is applied in practice as a material with limited flammability.

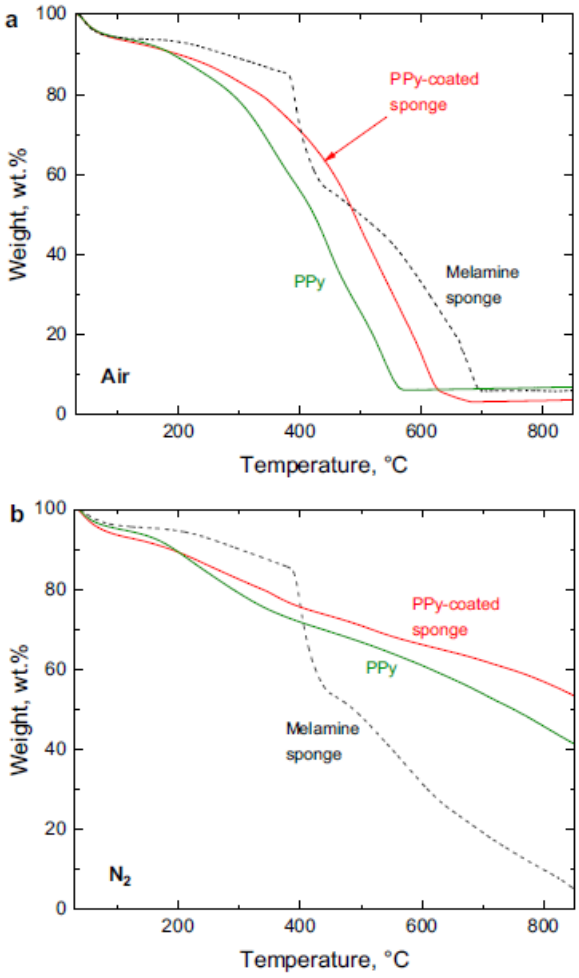

Fig. 7 Thermogravimetric analysis of melamine sponge (M-0, dashed line), polypyrrole and polypyrrole-coated sponge (M-1) a in air and b in nitrogen atmosphere

Compared with melamine, polypyrrole is less stable when heated in air (**Fig. 7a**). In contrast to melamine, however, polypyrrole gradually converts in inert atmosphere to a nitrogen-containing carbon (**Fig. 7b**) in good yield, e.g. 55 wt% of original mass at 700 °C. The amount of carbonized product still increased to 64 wt% for the polypyrrole-coated melamine sponge. This means that the polypyrrole coating becomes carbonized and prevents the degradation of underlying melamine interior. Such reasoning was used to explain the flame-retardancy in a similar system, polyaniline-coated cellulose fibres (Stejskal et al. **2005**), and could be applied in the design of flame-resistant polymer foams. The results also demonstrate the feasibility of the preparation of carbonized polypyrrole-coated melamine sponge as a novel macroporous nitrogen-enriched carbon (cf. the section below).

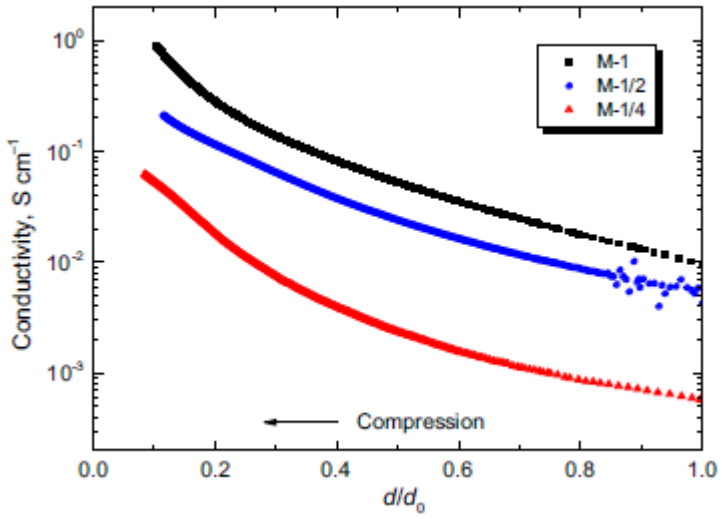

Fig. 8 The dependence of conductivity on the relative sample height, d/d_0

Specific surface area

The specific surface area of melamine sponge increased after the coating with polypyrrole (**Table 1**) but stayed at the order of several tens m^2g^{-1}. This is associated with the conversion of smooth melamine surface with fractal polypyrrole coating at low polypyrrole content (**Fig. 4**). The additional increase in polypyrrole content is due to the formation of free globular polypyrrole which has a specific surface area 13 m^2g^{-1} (Ruan et al. **2016**; Minisy et al. **2020a**). For that reason, the total specific surface area converges to this value, i.e. the specific surface area decreases with increase in polypyrrole loading (**Table 1**). The similar trend applies also to the pore volumes.

Conductivity

When the non-conducting sponge is uniformly coated with polypyrrole, the conducting phase within the macroporous composite is continuous. This is in the contrast to conventional composites, where the conducting phase is dispersed in the insulating matrix. The conductivity of the sponge was determined as a function of compression expressed as the relative change in the height of cylindrical sample, d/d_0. The starting height d_0 corresponds to a minimum applied pressure which was needed to provide a good contact o the sponge with electrodes. The conductivity increased as the samples

were compressed because the volume fraction of conducting component in the composite increased and the number of conducting pathways per infinitesimal sponge cross-section and the number of mutual contacts between them grew. The conductivity also increased with the polypyrrole loading (**Fig. 8, Table 1**) as expected and approached the conductivity of polypyrrole powder, which is close to 1 S cm^{-1} (Qiu et al. **2006**; Milakin et al. **2020**; Stejskal and Prokeš **2020**).

It is important to distinguish between the conductivity, σ (or resistivity, $\rho = 1/\sigma$), which is an intensive material characteristics, and the resistance, R, which is size- and shape-dependent property of the object. For practical pressure-sensitive applications, the resistance may be regarded as more important. The present data can be recalculated in formal way for the particular set-up represented by a cylindrical sample with the cross-section $S_c = \pi r^2$ (r = 5 mm) and height d as $R = \rho d/S_c$. The resistance of the samples decreased by 2-3 orders of magnitude when the sponge was compressed to ≈10% of its original length (**Fig. 9**).

Compressibility

The set-up used for the determination of conductivity *(cf.* the section above) allowed also for the assessment of mechanical properties of the sponges, because the dependence of the relative sample height on the applied pressure was monitored simultaneously (**Fig. 10**). When the reduction in the height d relative to the starting dimension d_0 is plotted in dependence on pressure, a double-logarithmic presentation is linear. The absolute value of the slope, $\Gamma = -\,d[\log(d/d_0)]/d(\log p)$ (**Table 1),** thus characterizes the pressure difference that is needed to produce a certain deformation. The higher is the slope, the easier the sponge is compressed.

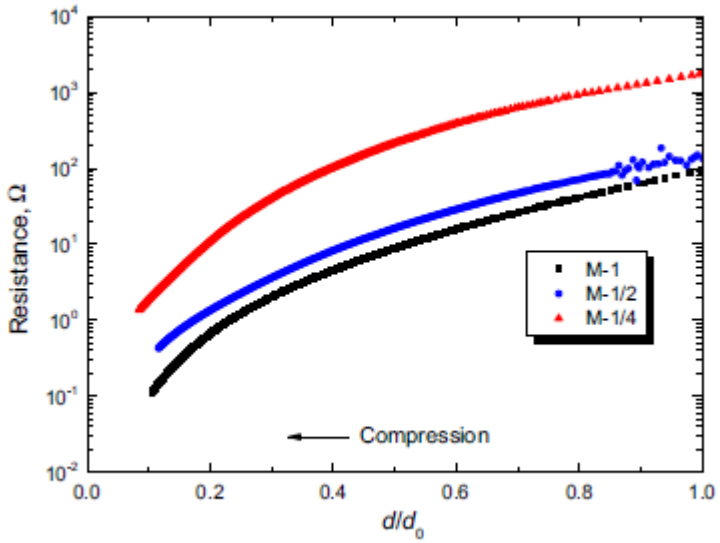

Fig. 9 The dependence of resistance on the relative sample height, d/d_0, for sponges with various polypyrrole content **(Table 1)**

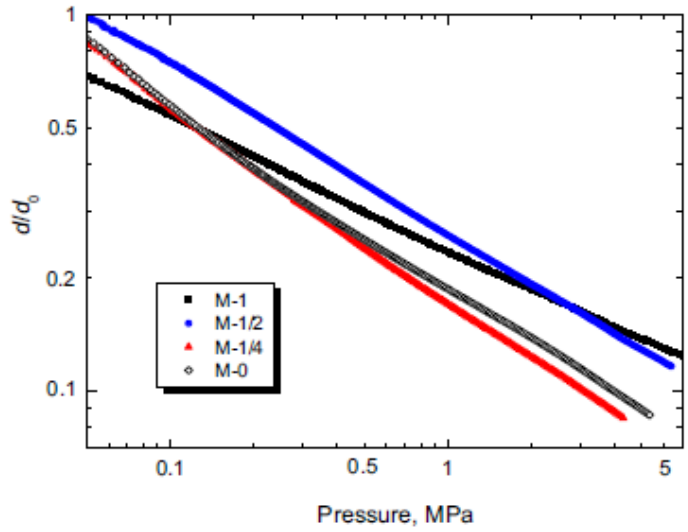

Fig. 10 The dependence of the relative sample height, d/d0, on the applied pressure for the sponges with various content of polypyrrole **(Table 1)**

The compressibility parameter Γ somewhat decreased after the coating with increasing amount of polypyrrole (**Table 1**), which can be interpreted as a stiffening of the sponge structure. This type of measurement also proves that the mechanical properties of melamine template have not been affected during polypyrrole deposition, which proceeds in aqueous medium under high acidity and in the presence of an oxidant.

Derived materials

Macroporous nitrogen-containing carbons

Melamine sponge coated with conducting polymers can serve as a new substrate for the preparation of macroporous nitrogen-containing carbons, a process illustrated so far on polyaniline (Gao et al. **2018**). The carbons obtained by the carbonization of polypyrrole alone (Ćirić-Marjanović et al. **2015**), and especially polypyrrole nanotubes (Chen et al. **2017**b; Stejskal and Trchová **2018**; Trchová and Stejskal **2018;** Stejskal et al. **2021b**) served in electrodes for supercapacitors (Raj et al. **2020**) or batteries (Chen et al. **2017**b; Lin et al. **2018**; Wu et al. **2018**), as catalyst support in fuel cells (Ozturk and Yurtcan **2018**), in desalination of water (Shi et al. **2020**) or as dye adsorbents in water-pollution treatment (Stejskal **2020**a; Stejskal et al. **2021**b). Melamine sponge alone is a rich source of nitrogen **(Fig. 1)** suitable for the morphology-retaining carbonization (Jing et al. **2020)**. Polypyrrole-coated melamine sponge is another substrate that was converted in this study to a macroporous nitrogen-containing carbon by heating in an electric oven to 650 °C at heating rate 10 °C min^{-1} under inert nitrogen atmosphere (**Fig. 11**).

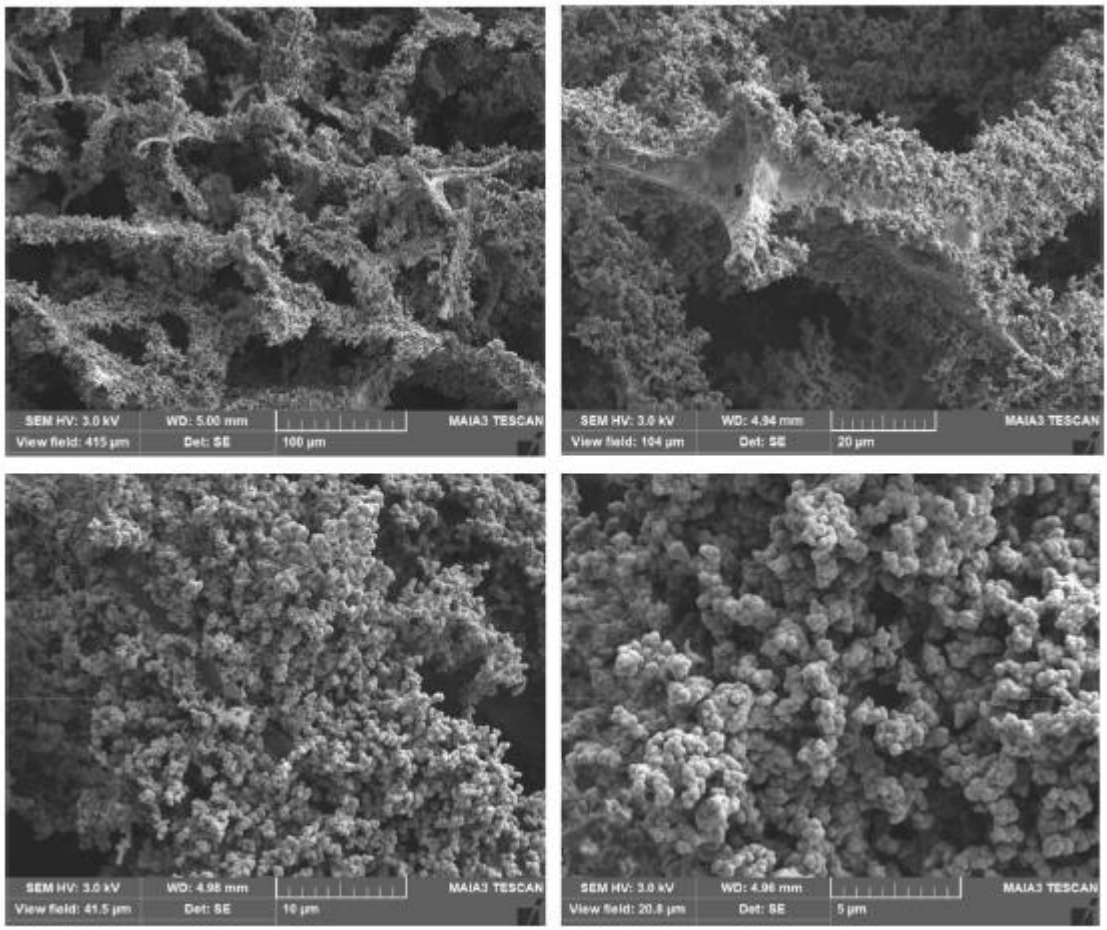

Fig. 11 Morphology of carbonized polypyrrole-coated melamine sponge observed at gradually increasing magnification (scale bars 100, 20, 10 and 5 µm)

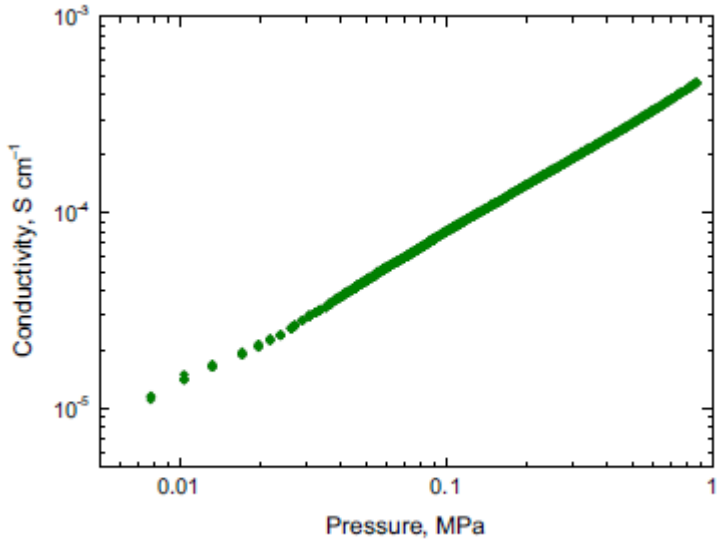

Fig. 12 Dependence of conductivity on pressure applied to a carbonized sponge (M-1)

Following the section on the thermogravimetric analysis, the feasibility of the carbonization was demonstrated by heating the polypyrrole-coated melamine sponge to 650 °C in inert atmosphere. Melamine alone is practically decomposed under such conditions, but after coating with polypyrrole, the yield was ≈65 wt% **(Fig. 7)**, i.e. sufficient for the carbonization at the preparative scale. The elemental analysis finds 55.3 wt% C, 1.6 wt% H and 23.9 wt% N, i.e. 2.3 C/N mass ratio, and calculated residual content 19.2 wt% O. The presence of chlorine from the hydrochloric acid constituting the salt with polypyrrole **(Fig. 2)** is unlikely because due to its volatility, it would leave the composite at the elevated temperature. The globular structure of the carbonized material observed at higher magnification is a result of the agglomeration of free polypyrrole globules ≈100 nm large that amalgamated at the carbonized sponge **(Fig. 11)**.

Raman spectra represent a powerful tool to follow the conversion of polypyrrole-coated melamine sponge to nitrogen-containing carbon at elevated temperature. The carbonized samples display two typical peaks located at 1600 and 1340 cm^{-1} assigned to graphitic (G) and disordered (D) modes, respectively (Pimenta et al. **2007**; Jorio et al. 2011) **(Fig. 6**). These bands have also been detected in infrared spectra (**Fig. 5**) due to the symmetry breaking of the structure.

The carbonized sponge introduces a specific macroporous material form suitable for applications. Nitrogen-containing carbons are potentially useful in the supercapacitors electrodes, as catalysts supports or adsorbents (Gao et al. **2018**; Ćirić-Marjanović et al. **2015**; Ozturk and Yurtcan **2018**). For some of them, a certain level of conductivity would be welcome. In the present case, the carbonized sponge had conductivity 1.1 x 10^{-5} S cm^{-1} that gradually increased to 4.6 x 10^{-4} S cm^{-1} after compression at ≈1 MPa **(Fig. 12)** when the sponge volume was reduced 10 x Globular polypyrrole carbonized under the same conditions had conductivity 2.1 x 10^{-3} S cm^{-1}.

Magnetic ferrosponge

Conducting polymers have sometimes been combined with magnetic materials represented by various iron oxides, such as maghemite (Minisy et al. **2020a**), magnetite (Qiu et al. **2006**; Pethsangave et al. **2020**) or ferrites (Kazantseva et al. **2004**; Bober et al. **2020**). Such composites can be separated by magnetic field when used, e.g., as adsorbents of organic dyes (Minisy et al. **2020**a; Bober et al. **2020**; Mashkoor and Nazar **2020**) or in their photocatalytic decomposition (Pethsangave et al. **2020**). Porous materials with a magnetic component are useful in biomedicine, when the sponge can be squeezed by applied magnetic field and thus used in the delivery of therapeutics (Ganguly and Margel **2020**). Such magnetic materials are often referred to as ferrosponges (Ganguly and Margel **2020**) even though they need not contain exclusively ferromagnetic components

The preparation of polypyrrole using the oxidation of pyrrole with iron (III) chloride **(Fig. 2)** (Kopecká et al. **2014)** offers a simple way how to introduce a magnetic component to this conducting polymer (Stejskal et al. **2021c)**. Iron(III) chloride in the polypyrrole preparation converts to iron(II) chloride (**Fig. 2**). If iron(III) chloride is used in stoichiometric excess, both chlorides accompany polypyrrole. After treatment with ammonium hydroxide, magnetite Fe_3O_4 is produced by co-precipitation method (Petcharoen and Sirivit **2012**; Chen et al. **2020**b; Mashkoor and Nazar **2020**; Stejskal et al. **2021**c) (**Fig. 13)**.

By using the strategy in the oxidation of 0.05 M pyrrole with 0.25 M iron(III) chloride (i.e. in excess of stoichiometric 0.125 M concentration, **Fig. 2**) followed by immersion in 1 M ammonium hydroxide, washing and drying, the magnetic and conducting melamine/polypyrrole/magnetite ferrosponge has recently been obtained (Stejskal et al. **2021**c) (**Fig. 14**). The coating with polypyrrole alone affords

only marginal magnetic properties due to contamination with iron compounds. The subsequent introduction of magnetite, however, endows the sponge with superparamagnetic properties **(Fig. 15**).

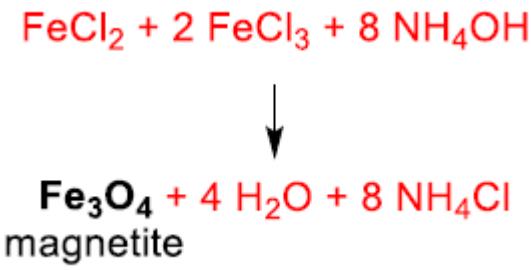

Fig. 13 Magnetite is produced from the mixture of iron(II) and iron(III) chlorides in ammonia solution

Fig. 14 Black polypyrrole-coated melamine sponge with deposited magnetite is attracted to a permanent magnet

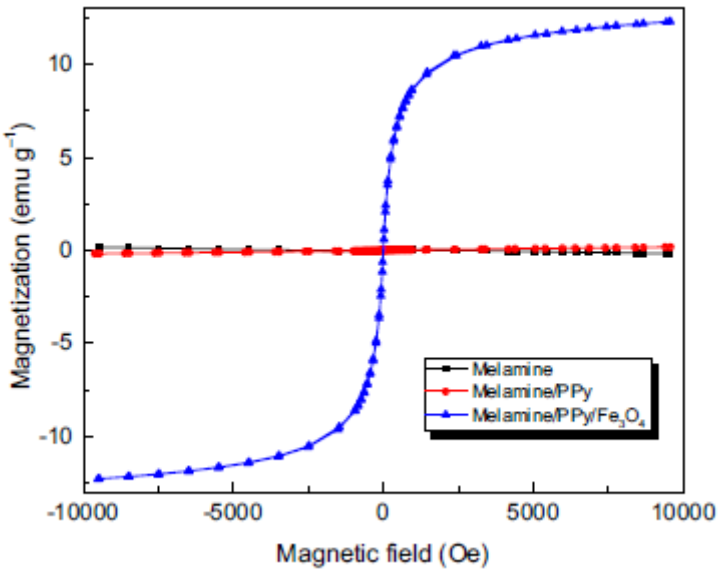

Fig. 15 Magnetization curves of the melamine sponge coated with polypyrrole (M/PPy) and this sponge after deposition of magnetite (M/PPy/Fe_3O_4). Melamine sponge alone (M) does not have any magnetic properties. Data from Ref. (Stejskal et al. **2021**c)

The sponge as a carrier of polypyrrole nanotubes

The standard preparation of polypyrrole gives rise to a globular polypyrrole. Any template in the reaction mixture becomes coated with a thin polypyrrole film with some adhering polypyrrole globules (**Fig. 4**).

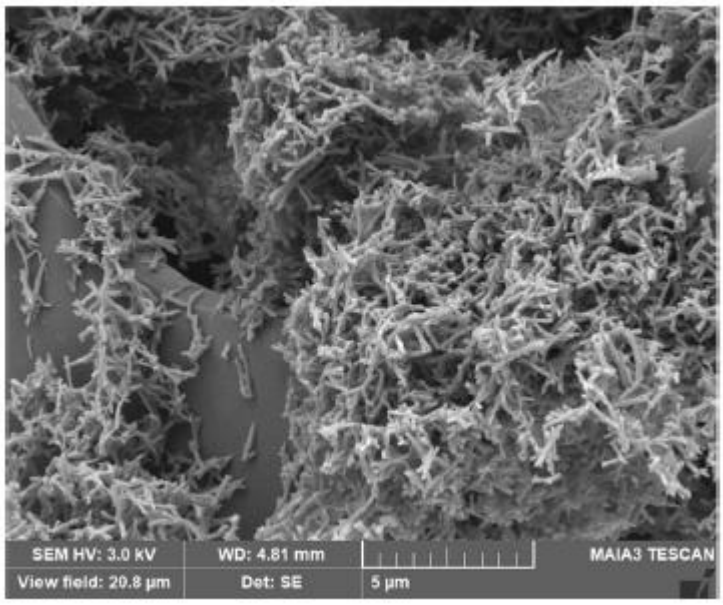

Fig. 16 Polypyrrole nanotubes deposited on melamine sponge (for details, see Ref. (Stejskal et al. **2021**d))

If the preparation protocol is modified to include 0.002 M methyl orange in the reaction mixture, the morphology of polypyrrole changes to distinctly nanotubular (Kopecká et al. **2014**; Stejskal **2018**; Li et al. **2020**b). Polypyrrole nanotubes were deposited on various surfaces, such as textile fibres (Bober et al. **2015**; Wei et al. **2017**; Wang et al. **2019**) and this applies in the present case also to melamine sponge (Stejskal et al. **2021**d) (**Fig. 16)**. Polypyrrole nanotubes have superior conductivity and improved stability with respect to deprotonation under physiological conditions (Stejskal et al. **2016**). This fact might be of interest in biomedical and environmental applications. Their superior performance after deposition on melamine sponge in the removal of organic dye from aqueous medium is demonstrated as follows.

Applications

Several applications of melamine sponges containing conducting polymers have already been mentioned the Introduction. In addition, bilayered polypyrrole/melamine foam was tested for the desalination of seawater by photothermal solar steam-generation (Li et al. **2019)**. Another study of polypyrrole-modified (Chen et al. **2017**a) or polyaniline-treated melamine sponge (Liu et al. **2015**) demonstrated the efficient oil/water separation in oil leakages causing the environmental pollution. Mass spectrometric monitoring of perfluorinated compounds involved polyaniline-modified sponge (Qi and Gong **2020**). Melamine sponge with electrochemically or chemically embedded polypyrrole served in flexible or compressible electrochemical capacitors (Chang et al. **2017**a, **2017b**, **2019**; Sun et al. **2019**; Liu et al. **2019**). The feasibility of additional applications, however, can also be illustrated.

It has to be again stressed that the deposition of conducting polymers reported in the literature took place in two steps, when the sponge penetrated with a monomer was transferred to the oxidant solution or vice versa. Under such conditions, both reactants meet at the surface of the sponge. The conducting polymer is thus formed preferentially there, while it may be absent in the sponge interior, i.e. the distribution of conducting polymer within the sponge is not even (Stejskal **2017**). The present study uses a novel way based on the single-step immersion in the solution containing both reactants that affords the uniform coating of the sponge.

Deformation-sensitive materials

The deformation of conducting foam-like materials, e.g., composites of carbonaceous and polymer foams, aerogels, or highly porous networks, by applied pressure is likely to induce changes in their electrical properties, viz. conductivity, resistance, capacitance, impedance, etc., as indeed observed **(Figs. 8, 9)**. One of the most accessible electrical quantity is the resistance. Hence, piezoresistive sensing of physical quantities, etc., pressure, force, strain, displacement, acceleration, etc., is the first obvious application of melamine sponges modified with a conducting polymer (Duan et al. **2019**; Chen et al. **2020**c; Stejskal et al. **2021**d). Sensitive sensing of low pressures is demonstrated below by a simple sensor based on melamine sponge containing polypyrrole **(Fig. 17)**.

A cylinder having 19.5 mm diameter and 60 mm length has been cut out from sponge (M-1/2). The cylinder was subsequently inserted into the optically transparent plastic tube of the same inner diameter directing the compression and expansion of the sponge **(Fig. 17a)**. Two phosphor bronze round electrodes were placed on the bottom and on the top of the sponge in the cylinder, respectively. A four-wire connection allowing to measure low resistance has been used for

continuous AC measurement (voltage 1 V, frequency 1 kHz, C-R mode) of parallel resistance R of the cylinder (**Fig. 17a**) with a LCR-6002 (GW-Instek, USA).

The pressure sensor was placed under the Sauter TVL testing stand equipped by force gauge Sauter FH50 creating a maximum force of 50 N with a resolution of 0.01 N **(Fig. 17b**). The magnitude of compression and expansion was measured by an in-built deflection gauge with a resolution of 10 µm. The pressure P acting on the sensor was calculated using formula *P=F/A*, where *F* is the force measured by force gauge and A is an in-plane cross-sectional area of the sponge cylinder.

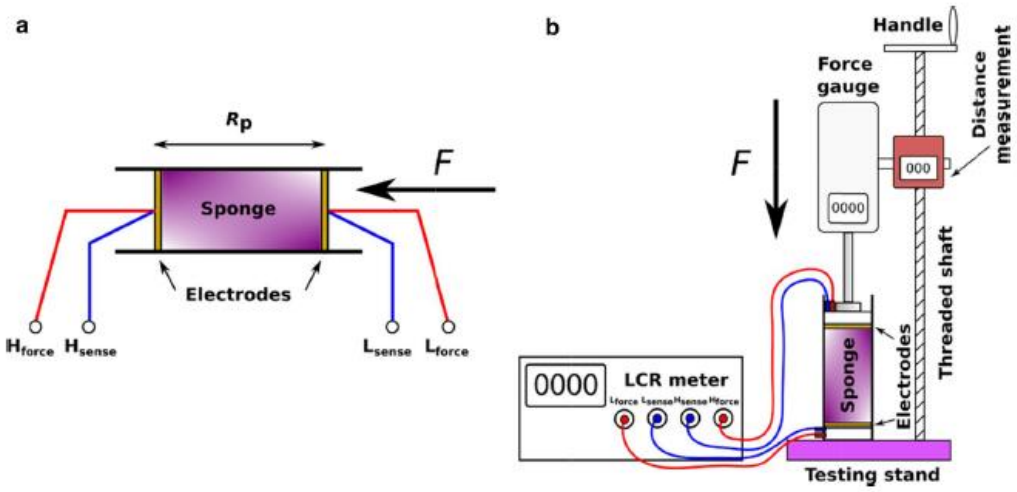

Fig. 17 a The pressure sensor and b simplified scheme of the testing apparatus

At first, static properties of the pressure sensor in the form of a characteristic curve have been evaluated **(Fig. 18a**). The curve provides the basic information about the sensitivity, range and hysteresis of the sensor. The characteristic curve (**Fig. 18a**) clearly indicates nonlinear static properties of the sensor with the highest sensitivity at low pressures. The most significant change in the resistance, over two orders of magnitude, is in the range of 0-10 kPa. The measuring range of the sensor was tested up to 135 kPa. The use of relatively high pressures exceeding 10 kPa creates a significant "memory effect" of the sponge as indicated by red curve of decreasing pressure (**Fig. 18**a). The sponge returns to its initial shape after applying extreme pressures in the maxima of the measuring range > 10 kPa only slowly. However, when moderate pressures are used, < 10 kPa, the process of repeated compression and expansion is immediate and reversible without undesired "memory effect" (**Fig. 18b)**.

The presented proof of concept for the pressure sensor based on melamine sponge coated by polypyrrole can be summarized in several points: (1) the sensor has a nonlinear characteristic common to, e.g., capacitive pressure sensors used in the industry (Kadlec et al. **2019**); (2) the sensor is designed for sensitive measurement of relatively low pressures up to 10 kPa and it can therefore be used, e.g. in tactile and wearable sensors (Lu et al. **2019**); (3) the sensor suffers from the memory effect when its working range is substantially exceeded, but when operated within the working range (< 10 kPa), its response is negligibly affected by repeated compression and expansion; (4) the sensor can be prepared relatively easily and inexpensively.

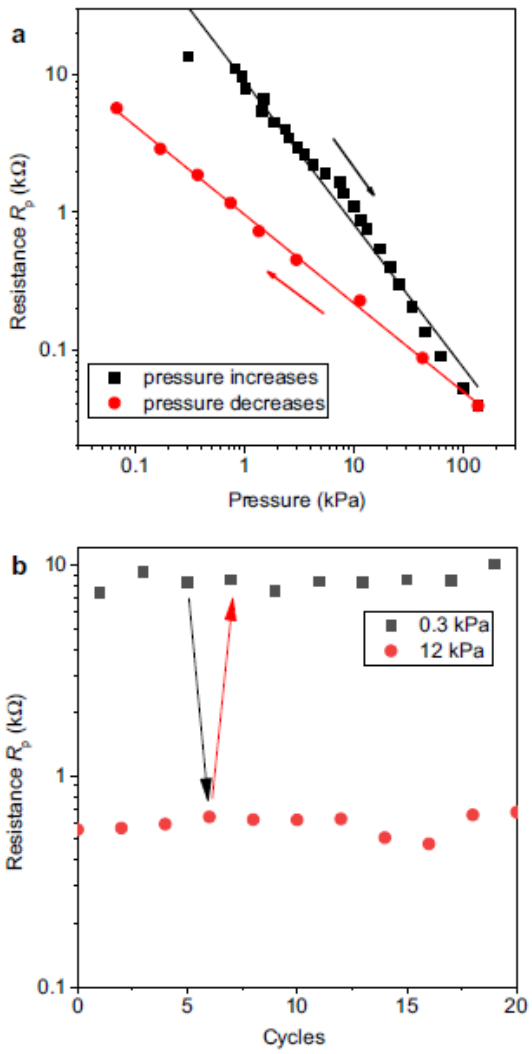

Fig. 18 a The double-logarithmic presentation of the characteristic curve of the pressure sensor and b the repeated compression/expan-sion cycling

Electromagnetic radiation shielding

The materials incorporating conducting polymers have often been reported in the literature to shield electromagnetic radiation (Chen et al. **2020**b; Moučka et al. **2021**; Stejskal et al. **2021**a, **2021**d). For example, the composite of polypyrrole-coated multi-wall carbon nanotubes embedded in polyurethane matrix proved to be efficient shielding material in GHz frequency region (Gahlout and Choudhary **2020**). The shielding efficiency in the composite using polydimethyl-siloxane depended also on the polypyrrole nanostructure (Moučka et al. **2020, 2021**).

Electromagnetic radiation shielding parameters of sponges were determined with the PNA-L Network Analyser Agilent N5230A (Agilent Technologies, Santa Clara, CA, USA). The frequency range of the vector network analyser was 5.85 to 8.2 GHz. The shielding of electromagnetic radiation shielding is usually described in terms of two parameters. While Sn describes the portion of reflected

radiation, S21 gives direct information on transmitted radiation through the sample of given thickness (Varsheny and Dhawan **2017**) (**Fig. 19**).

The shielding parameters S11 and S12 are little dependent on frequency in GHz region (**Fig. 19**). The same consequently applies to the absorbance, transmittance and reflectance of composite sponges **(Fig. 20)**. The shielding afforded by melamine sponge alone is negligible. The transmittance steadily decreases in dependence on polypyrrole loading as expected. The presence of polypyrrole is clearly responsible for the observed radiation absorbance, which is virtually independent of the polypyrrole content. The reflectance, on the other hand, increases with increasing polypyrrole content. Polypyrrole is present in the sponge in two forms: (1) as a coating of melamine threads, which is independent on the overall polypyrrole content and (2) as polypyrrole nanoparticles acting as a relatively free-flowing filler of macropores, which may represent the majority of polypyrrole. We can thus speculate that polypyrrole coating participates especially in the radiation absorption, while a high surface area of polypyrrole nanoparticles contributes to the radiation reflection. The shielding afforded by various polypyrrole nanostructures differs (Moučka et al. 2020), and this applies also to polymer coatings and nanoparticles.

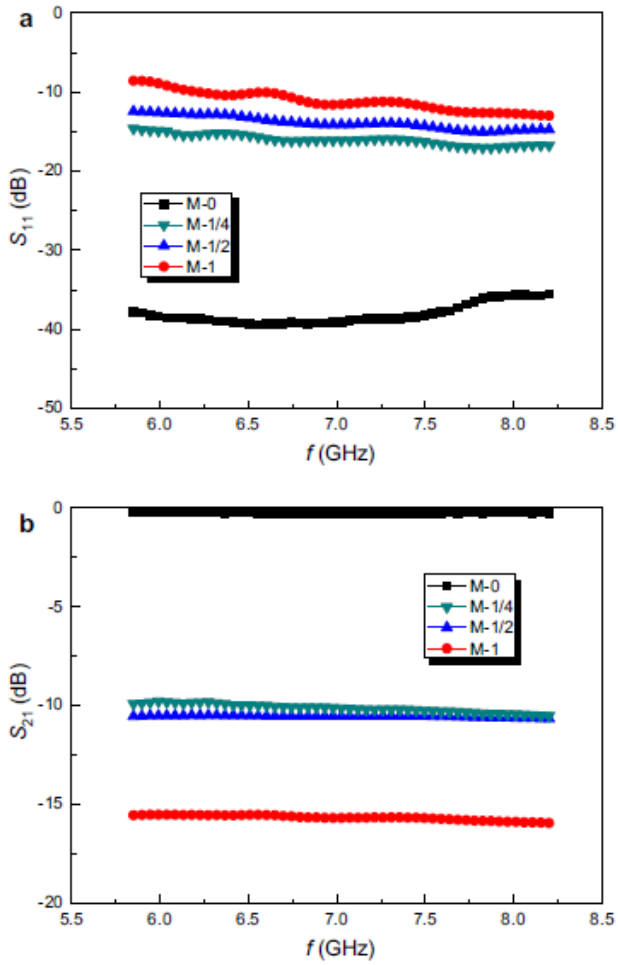

Fig. 19 Frequency dependence of a a forward reflection coefficient Sjj and b a reverse transmission coefficient S21 for sponges containing various fractions of polypyrrole (**Table 1)**

Electrically heated sponge

The composites based on conducting polymers are well suited for the generation of Joule heat by passing current (Wu et al. **2021**). Polypyrrole-coated polyethylene tereph-thalate fabrics (Sparavigna et al. **2010**) or polyester wipers (Xie et al. **2020**) were used for the heat generation by passing current, and the temperature increase in the substrate to 70-90 °C was reported. This approach has recently been extended to the sponge coated with polypyrrole (Wu et al. **2021**) and some properties of such material are reported also as follows (**Fig. 21**).

Depending on applied voltage, the temperature increased until the generated heat balanced the heat dissipation (**Fig. 22**). Temperature exceeding 150 °C was easily reached in a few minutes.

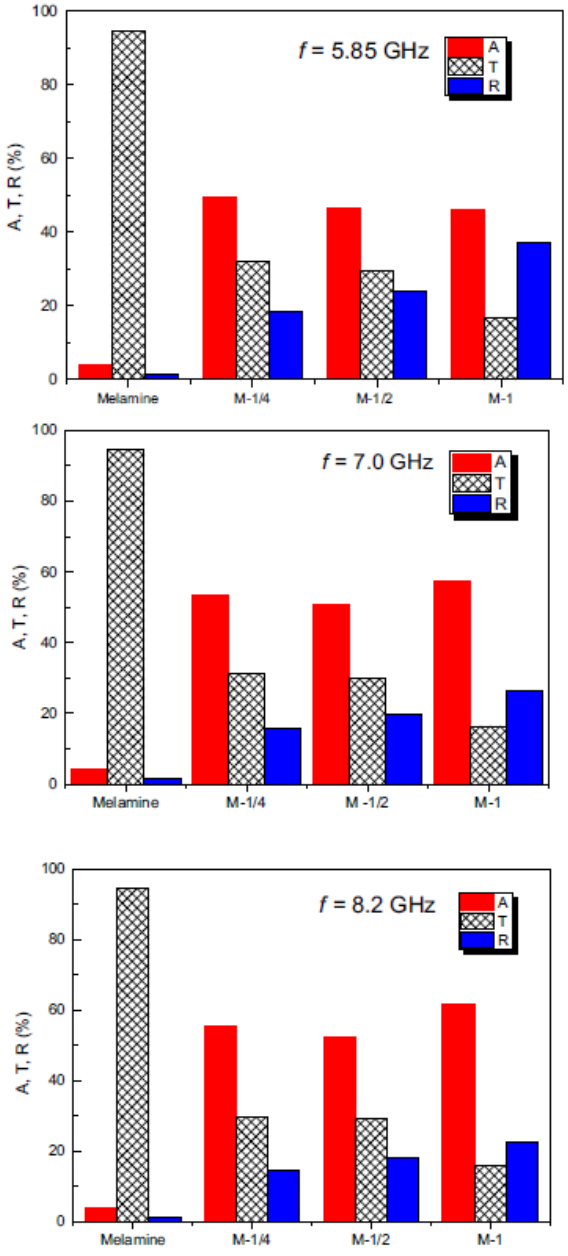

Fig. 20 Absorbance A, transmittance T, and reflectance R of melamine sponge and the sponges containing various amounts of polypyrrole (**Table 1**) at 5.85, 7.0 and 8.2 GHz frequency

In the next experiment, the sponge was heated in 5 min to 80 °C and the voltage was switched off (Fig. 23). The time needed for the temperature to become close to laboratory conditions was longer, about 45 min, as expected for the thermally insulating sponge. The voltage was then switched on again and the heating could be repeated with a good reproducibility. Melamine sponges are used in practice as a thermal insulation. Polypyrrole-modified sponge applied as a heated insulation material would probably make sense.

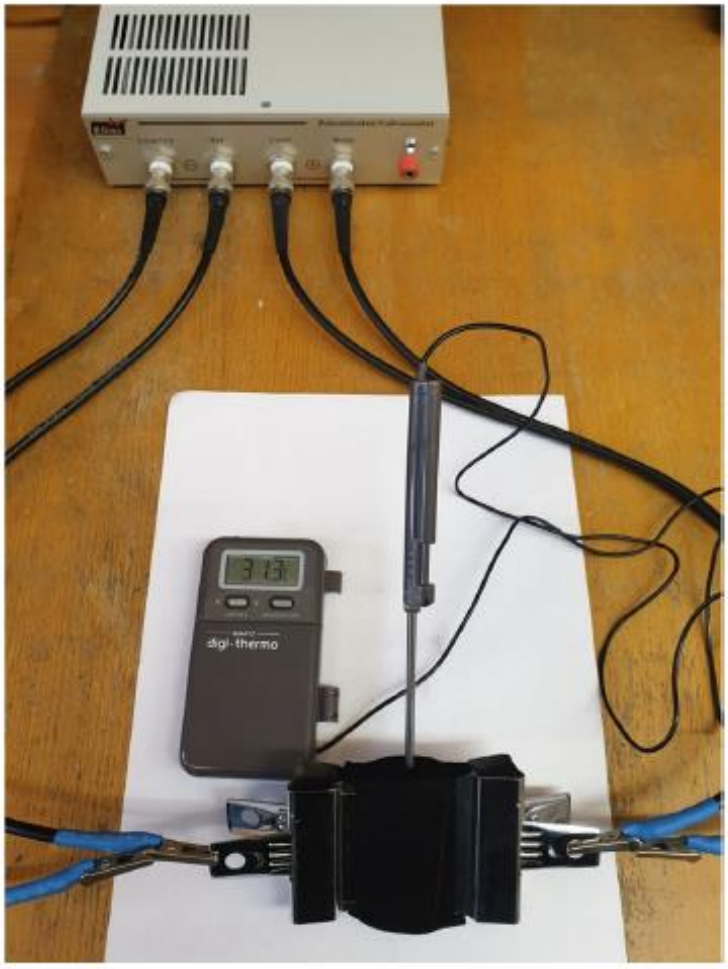

Fig. 21 The DC voltage was applied to the sponge containing 40 wt% polypyrrole (M-1/2) using steel clamps. Temperature inside the sponge was recorded by a digital thermometer

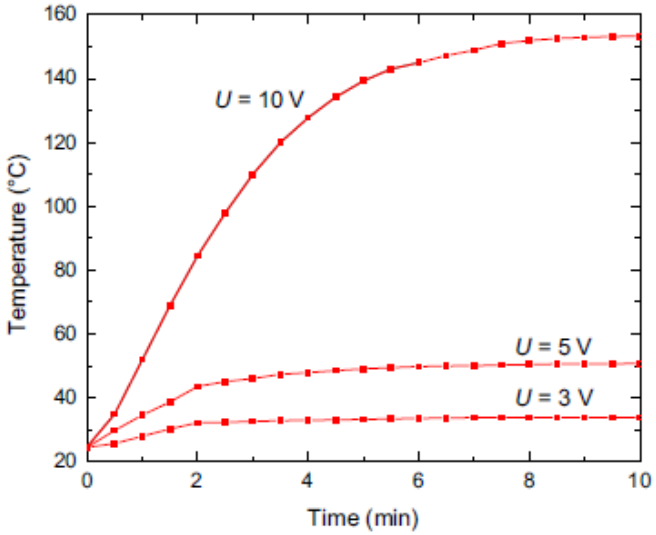

Fig. 22 The time dependence of sponge temperature at various applied voltages, U

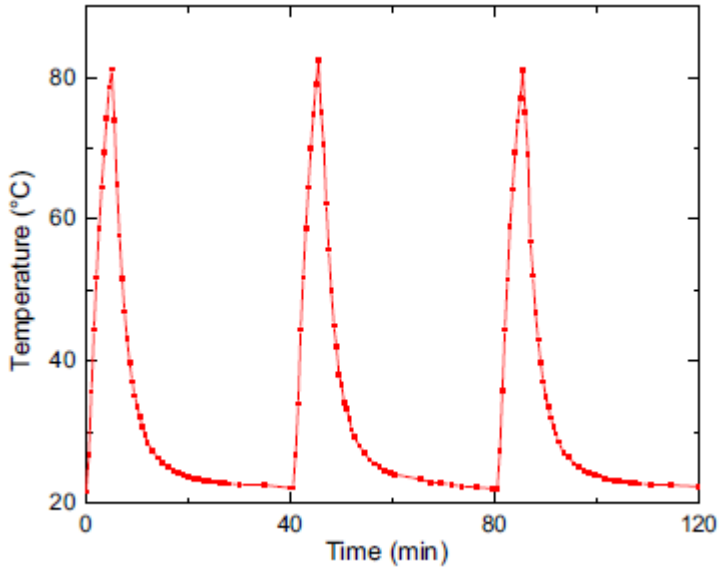

Fig. 23 The temperature profile during the repeated on/off heating cycles. U=7 V

Cytotoxicity

Application of conducting polymers in biomedicine is highly topical due to their organic character and mixed electronic and ionic conductivity (Zare et al**. 2020**). Polypyrrole is especially interesting thanks to advantageous stability of the conductivity under physiological conditions (Stejskal et al. **2016**). It was previously demonstrated that biocompatibility of polypyrrole is not limited by cytotoxicity compared with other conducting polymers (Humpolíček et al. **2018**; Capáková et al. **2020**).

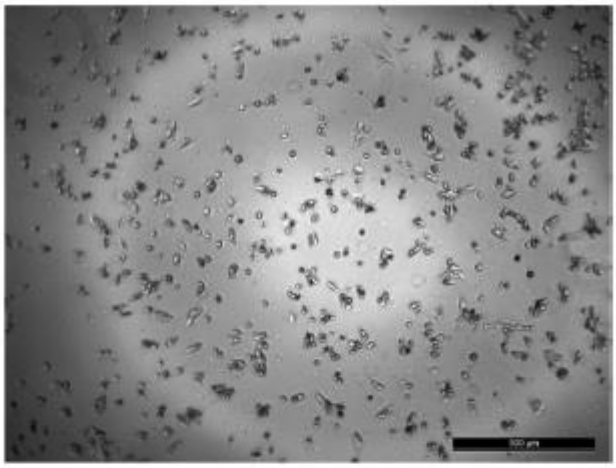

Melamine sponge

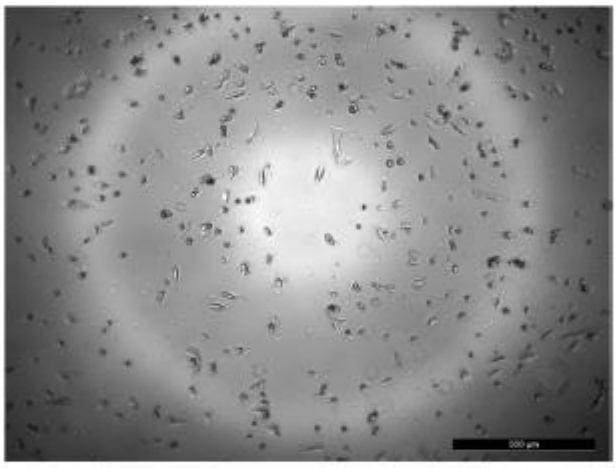

Polypyrrole-coated melamine sponge

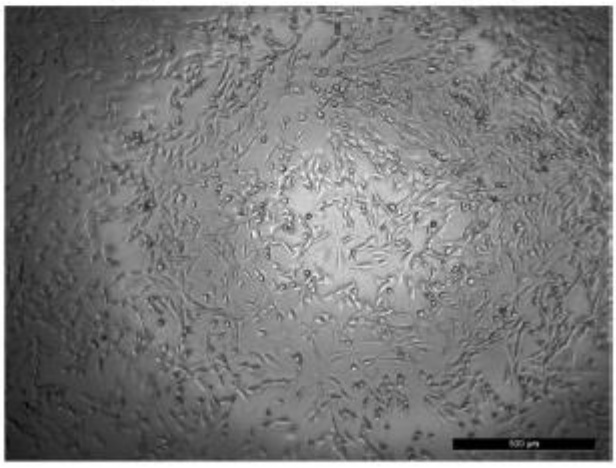

Reference

Fig. 24 Example of cytotoxicity displayed by parent extracts of native melamine sponge, melamine sponge coated with polypyrrole and reference

The fundamental limitation of application of conducting polymers in biomedicine is the inability to form solid structures by themselves. For that reason, the coating of suitable templates, here a macroporous sponge, with conducting polymer may be a solution. To express the potential use of melamine sponge as a carrier for preparation of threedimensional macroporous conducting material for biomedical purposes, the cytotoxicity was determined on both the native melamine sponge and melamine sponge coated by polypyrrole. To demonstrate the effect of extracts on the cells, their morphology when cultivated in parent 100% extract was visualized (**Fig. 24**). It is clearly seen that parent extract has a harmful effect on the cells.

The visualization of cells incubated in presence of extracts is certainly only informative. More important is the quantitative analysis of cell viability (Fig. 25). The decrease in viable cells to less than 70% compared with reference can be considered as potentially cytotoxic. Here, the extracts above the 25% dilution reached this level. This is, however, comparable to neat polypyrrole (Humpolíček et al. 2018). More important is the fact that the coating of melamine sponge with polypyrrole does not increase the cytotoxicity potential. The cytotoxicity is therefore inherent to the carrier melamine sponge rather than to the polypyrrole coating.

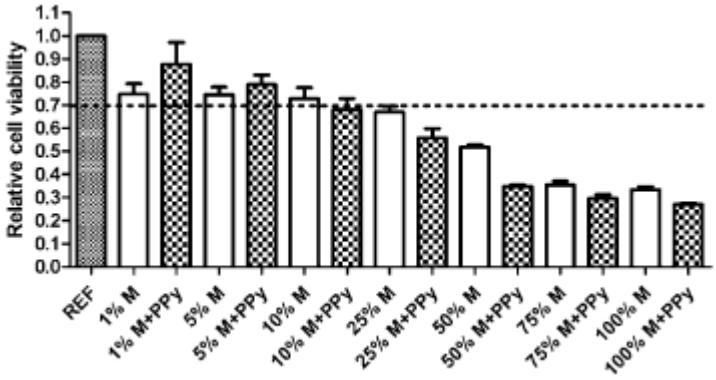

Fig. 25 The cytotoxicity of extracts of native melamine sponge (M) and melamine sponge coated with polypyrrole (M + PPy; sample M-1)

This is probably due to a sodium bisulfite component present in the commercial product. While this may restrict some uses of foams as scaffolds in tissue engineering, in antibacterial decontamination of water, this would be of benefit (Ivanova et al. **2017**).

Adsorption of organic dye

Conducting polymers and their substituted derivatives and composites have frequently been used as efficient adsorbents of organic dyes in water-pollution treatment (Dutta and Rana **2019**; Sapurina et al. **2020**; Stejskal **2020a**). This application exploits the similarity of conducting polymers and organic dyes that share the conjugated molecular structure and the presence of aromatic rings. For example, Reactive Black 5 (**Fig. 26**) was used to demonstrate this fact with the composites based on polyaniline (Janaki et al. **2013**; Ballav et al. **2015**; Bhaumik et al. **2015**), poly(p-phenylenediamine) (Minisy et al. **2020b**) or polypyrrole (Díaz-Flores et al. **2019**; Stejskal et al. **2021**d). In the contrast to common adsorbents, electrical and electrochemical properties of conducting polymers are of benefit (Stejskal **2020b**). For example, the dye adsorption can be affected by electric potential (Haque and Wong

2017) and the same principle was applied in the controlled drug delivery (Caldas et al. 2020) or in electrooxidative (Liu et al. 2020) and electrocatalytic (Maldonado-Larios et al. 2020) removal of

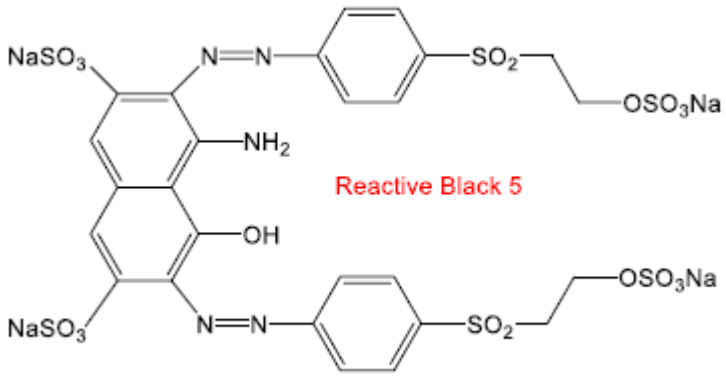

Fig. 26 Reactive Black 5 delivery (Caldas et al. **2020**) or in electrooxidative (Liu et al. **2020**) and electrocatalytic (Maldonado-Larios et al. **2020**) removal of pollutant dyes.

In dye-adsorption studies, conducting polymers have been used alone as powders but more often they were deposited on suitable substrates that provide desirable mechanical and structural materials properties. A commercial macroporous open-cell melamine sponge makes a promising template for the deposition of a conducting polymer meant to be applied in adsorption of pollutant organic dyes. It has recently been demonstrated for Reactive Black 5 that the globular polypyrrole is poor dye adsorbent in the contrast to polypyrrole nanotubes (Stejskal et al**. 2021b, 2021d**). For that reason, polypyrrole nanotubes were deposited on melamine sponge (cf section above) and tested for adsorption of anionic dye, Reactive Black 5.

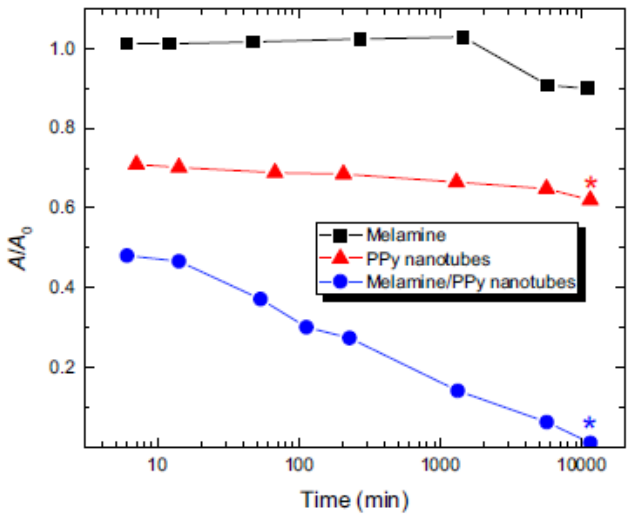

Fig. 27 Time dependence of the relative decrease in the optical absorbance of Reactive Black 5 solution (0.1 mg mL^{-1}) at 598 nm after addition of melamine sponge (80 mg), polypyrrole nanotubes (20 mg) or of polypyrrole/melamine sponge (100 mg; M-1/4). Asterisks denote the cases shown in **Fig. 28**

The results indicate that melamine sponge alone does not adsorb this dye (**Fig. 27**). Polypyrrole nanotubes used as a powder adsorbed immediately (within 3-5 min) about a quarter of available dye but further changes in the dye concentration were marginal. On the other hand, melamine sponge with deposited polypyrrole nanotubes removed quickly about one half of a dye and then, more slowly, adsorbed the rest (**Fig. 27**) until no visible coloration of aqueous phase was seen **(Fig. 28)**. The experiment illustrates the importance of polypyrrole nanomorphology, as well as the role of carrier substrate used for the conducting polymer deposition. For the practical applications, however, the interaction with other dyes has to be also investigated.

Fig. 28 Even after 2 weeks, the solution of Reactive Black 5 with polypyrrole nanotubes stays coloured (left, cf**. Figure 27**). When polypyrrole nanotubes were deposited on melamine sponge, the dye removal was practically complete (right)

Reductive deposition of silver nanoparticles

Polypyrrole is able to reduce noble-metal ions to corresponding metals (**Fig. 29**). This approach has been extensively used for the deposition of silver nanoparticles on polypyrrole and its composites (Stejskal **2013**). The resulting composite materials have been tested in solar-driven distillation of water (Xu et al. **2020**) and especially in antibacterial compositions (Maráková et al. **2017**; Mahlangu et al. **2019**; Zhang et al. **2020**). The deposition of noble-metal nanoparticles, viz. platinum, palladium, rhodium and ruthenium, on polypyrrole nanotubes has been also demonstrated and applied in the heterogeneous catalysis (Sapurina et al. **2016**).

The feasibility of silver deposition at polypyrrole-coated melamine sponge can be qualitatively demonstrated by its immersion in the 0.1 wt% aqueous solution of silver nitrate for 5 days followed by rinsing with water until no silver ions have been detected. Silver particles appear in micrographs as white spots of sub-micrometre size with broad particle-size distribution (**Fig. 30**). The prolonged deposition procedure, however, led to the damage of the sponge structure and individual threads broke. This could be prevented by the shortening of deposition time.

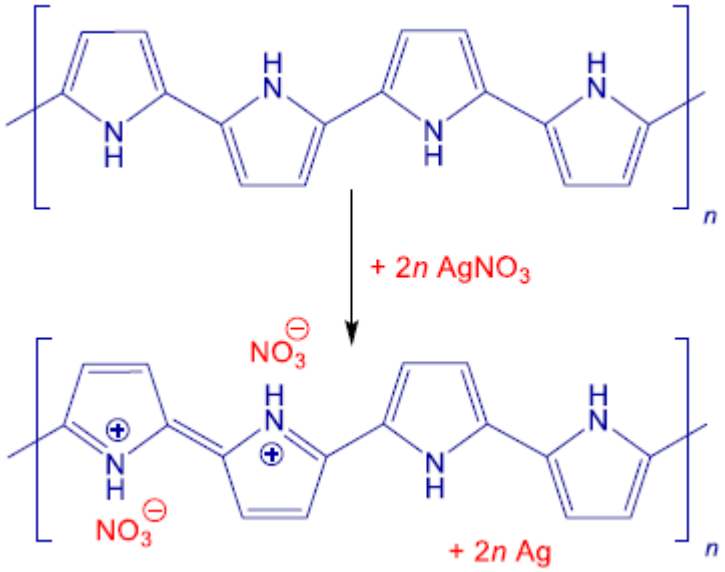

Fig. 29 Silver nitrate is reduced with polypyrrole base to metallic silver

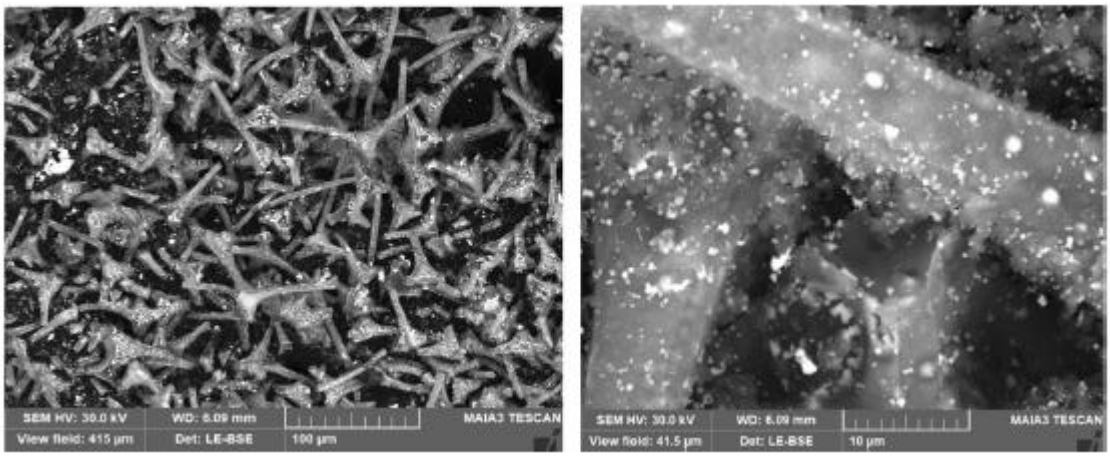

Fig. 30 Melamine sponge coated with polypyrrole (M-1/2) with deposited silver nanoparticles taken in back-scattered electrons mode at lower (left) and higher magnification (right)

Conclusions and outlook

The coating of melamine sponge with conducting polypyrrole demonstrates the preparation of macroporous conducting material with a broad application potential. For the successful preparation, the sponge has to be penetrated with freshly prepared aqueous solutions of pyrrole and oxidant, iron(III) chloride, i.e. not by successive treatment with reactant solutions. The contact with reaction mixture should be reduced to tens of minutes to prevent the potential degradation of template sponge. The concentration of reactants should be as low as possible to avoid the formation of free

polypyrrole in addition to polymer coating, i.e. below ≈20 wt% relative to the sponge mass. The sponges have open-cell macroporous structure that distinguish them from closed-cell microporous hydrogels based on conducting polymers (Stejskal **2017**; Tomczykowa and Polonska-Brzezinska **2019**; Li et al. **2021**). The conversion of polypyrrole-coated sponges to nitrogen-containing carbons or magnetic ferrosponges is illustrated, as well as examples of potential applications of macroporous conducting materials.

Polypyrrole-modified sponges could be applied in directions where three-dimensional structure would be of benefit (Chen et al. **2020c**; Ganguly and Margel **2020**; Zare et al. **2020**). The mixed ionic and electronic conductivity (Stejskal et al. **2009**) make conducting polymers as materials of choice for the interfaces operating between systems with these conductivity types, e.g., between stimulating or monitoring electrodes for biological objects or electrodes in batteries, but also in other energy-conversion devices. Despite being a conducting polymer, electrical properties need not be of prime interest (Stejskal **2020**b). Polypyrrole can perform the chemical role as a reductant of noble-metal compounds to corresponding metal nanoparticles (Stejskal **2013**; Sapurina et al. **2016;** Maldonado-Larios et al. **2020**), followed by application in heterogeneous catalysis of organic reactions or in the recovery of noble metals. Conducting polymers are flame-retardant, which would be a welcome property when used in heating applications. The combination of sound absorption, antistatic coatings and reduced flammability might be of interest to automotive industry. In water-pollution treatment, the sponges modified with conducting polymers can be used for the removal of organic dyes and heavy-metal ions from water (Stejskal **2020**a; Sapurina et al. **2020**). The coating of hydrophobic sponge with a conducting polymer can convert its surface to hydrophilic one, and the contact angle could be varied (Stejskal et al. **2008**). The electroactivity of conducting polymers could be exploited in the control of adsorption processes by applying electrical potential (Baptista et al. **2021**; Xu et al. **2021**). In extended studies, polypyrrole can be replaced with polyaniline or polymers of ring-substituted aniline derivatives, e.g. polyphenylenediamines (Stejskal **2015**). The research and application potential of macroporous polymer materials modified with conducting polymers is thus quite promising.

References

Antonio-Carmona ID, Martínez-Amador SY, Martínez-Gutiérrez H, Ovando-Medina VM, González-Ortega O (2015) Semiconducting polyurethane/polypyrrole/polyaniline for microorganism immobilization and wastewater treatment in anaerobic/aerobic sequential packed bed reactors. J Appl Polym Sci 132:42242. https://doi.org/10.1002/app.42242

Ballav N, Debnath S, Pillay K, Maity A (2015) Efficient removal of reactive black from aqueous solution using polyaniline coated ligno-cellulose as a potential adsorbent. J Mol Liq 209:387-396. https://doi.org/10.1016/)'.molliq.2015.05.051

Baptista AC, Brito M, Marques A, Ferreira I (2021) Electronic control of drug release from gauze or cellulose acetate fibres for dermal applications. J Mater Chem B 9:3515-3522. https://doi.org/10. 1039/d1tb00249j

Bhaumik M, McCrindle RI, Maity A, Agarwal S, Gupta VK (2015) Polyaniline nanofibers as highly effective re-usable adsorbent for removal of reactive black 5 from aqueous solutions. J Colloid Interface Sci 466:442-451. https://doi.org/10.1016/j.jcis. 2015.12.056

Blinova NV, Stejskal J, Trchová M, Ćirić-Marjanović G, Sapurina I (2007) Polymerization of aniline on polyaniline membranes. J Phys Chem B 141:2440-2448. https://doi.org/10.1021/jp067370f

Bober P, Stejskal J, Šeděnková I, Trchová M, Martinková L, Marek J (2015) The deposition of globular polypyrrole and polypyrrole nanotubes on cotton textile. Appl Surf Sci 356:737-741. https:// doi.org/10.1016/j.apsusc.2015.08.105

Bober P, Minisy IM, Acharaya U, Pfleger J, Babayan V, Kazantseva N, Hodan J, Stejskal J (2020) Conducting polymer composite aerogel with magnetic properties for organic dye removal. Synth Met 260:116266. https://doi.org/10.1016/j7synthmet.2019.116266

Caldas M, Santos AC, Rebelo R, Pereira I, Veiga F, Reis RL, Correlo VM (2020) Electro-responsive controlled drug delivery from melanin nanoparticles. Int J Pharm 558:119773. https://doi.org/ 10.1016/j.ijpharm.2020.119773

Capáková Z, Radaskiewicz KA, Acharya U, Truong TH, Pacherník J, Bober P, Kašpárková V, Stejskal J, Pfleger J, Lehocký M, Humpolíček P (2020) The biocompatibility of polyaniline and polypyrrole 2: Doping with organic phosphonates. Mater Sci Eng C 113:110986. https://doi.org/10.1016/j.msec.2020.110986

Chang YH, Han GY, Xiao YM, Chang YZ, Song H, Li MY, Li YP, Zhang Y (2017a) Internal tandem flexible and compressible electrochemical capacitor based on polypyrrole/carbon fibers. Electrochim Acta 257:335-344. https://doi.org/10.1016/j.elect acta.2017.10.106

Chang YH, Han GY, Chang YZ, Xiao YM, Hou WJ, Zhou W (2017b) Flexible and compressible electrochemical capacitors based on polypyrrole/carbon fibers integrated into sponge. J Alloy Comp 708:1206-1215. https://doi.org/10.1016/j.jallcom.2017.03.107

Chang YH, Wang N, Han GY, Li MY, Xiao YM, Li HG (2019) The properties of highly compressible electrochemical capacitors based on polypyrrole/melamine sponge-carbon fibers. J Alloy Comp 786:668-676. https://doi.org/10.1016/joallcom.2019.01. 365

Chen JC, You H, Xu LQ, Li TH, Jiang XQ, Li CM (2017a) Facile synthesis of two-tier hierarchical structured superhydrophobic-superoleophilic melamine sponge for rapid and efficient oil/water separation. J Colloid Interface Sci 506:659-668. https://doi.org/ 10.1016/j.jcis.2017.07.066

Chen XF, Huang Y, Zhang KC, Feng XS, Wang MY (2017b) Synthesis and high-performance of carbonaceous polypyrrole nanotubes coated with SnS2 nanosheets anode materials for lithium ion batteries. Chem Eng J 330:470-479. https://doi.org/10.1016/j.cej. 2017.07.180

Chen JL, Xue FQ, Yu ZH, Huang LT, Tang DP (2020a) A polypyr-role-polydimethylsiloxane sponge-based compressible capacitance sensor with molecular recognition for point-of-care immunoassay. Analyst 145:7186-7190. https://doi.org/10.1039/d0an0 1653e

Chen XL, Shi T, Wu GL, Lu Y (2020b) Design of molybdenum disulfide@polypyrrole composite decorated with Fe3O4 and superior electromagnetic wave absorption performance. J Colloid Interface Sci 572:227-235. https://doi.org/10.1016/j.jcis. 2020.03.089

Chen W, Yan X (2020) Progress in achieving high-performance piezoresistive and capacitive flexible pressure sensors: a review. J Mater Sci Technol 43:175-188. https://doi.org/10.1016/j.jmst. 2019.11.010

Ćirić-Marjanović G, Pašti I, Gavrilov N, Janosevic A, Mentus S (2015) Carbonised polyaniline and polypyrrole: towards advanced nitrogen-containing carbon materials. Chem Pap 67:781-813. https:// doi.org/10.2478/s11696-013-0312-1

Díaz-Flores PE, Guzmán-Alvarez CJ, Ovando-Medina VM, Mar-tínez-Gutiérrez H, González-Ortega O (2019) Synthesis of a-cellulose/magnetite/polypyrrole composite for the removal of reactive black 5 dye from aqueous solutions. Desalin Water Treat 155:350-363. https://doi.org/10.5004/dwt.2019.24013

dos Santos MR, Alcaraz-Espinoza JJ, da Costa MM, de Oliveira HP (2018) Usnic acid-loaded polyaniline/polyurethane foam wound dressing: preparation and bactericidal activity. Mater Sci Eng C 89:33-40. https://doi.org/10.1016/jmsec.2018.03.019

Duan L, D'Hooge DR, Cardon L (2019) Recent progress on flexible and stretchable piezoresistive strain sensors: from design to application. Prog Mater Sci 114:100617. https://doi.org/10. 1016/j.pmatsci.2019.100617

Dutta K, Rana D (2019) Polythiophenes: an emerging class of promising water purifying materials. Eur Polym J 116:370-385. https:// doi.org/10.1016/j.eurpolymj.2019.04.033

Fedorova S, Stejskal J (2002) Surface and precipitation polymerization of aniline. Langmuir 18:5630-5632. https://doi.org/10.1021/ la025665o

Feng Y, Yao JF (2018) Design of melamine sponge-based three-dimensional porous materials toward applications. Ind Eng Chem Res 57:7322-7330. https://doi.org/10.1021/acs.iecr.8b01232

Gahlout P, Choudhary V (2020) EMI shielding response of polypyr-role-MWCNT/polyurethane composites. Synth Met 266:116414. https ://doi.org/10.1016/j. synthmet.2020.116414

Ganguly S, Margel S (2020) Review: remotely controlled magnetoregulation of therapeutics from magneto elastic gel matrix. Bio-technol Adv 44:107611. https://doi.org/10.1016/j.biotechadv. 2020.107611g

Gao ZY, Zhang LC, Chang JL, Wang Z, Wu DP, Xu F, Guo YM, Jiang K (2018) Catalytic electrode-redox electrolyte supercapacitor system with enhanced capacitative performance. Chem Eng J 335:590-599. https://doi.org/10.1016/jxej.2017.11.037

Gu WH, Tan JW, Chen JB, Zhang Z, Zhao Y, Yu JW, Ji GB (2020) Multifunctional bulk hybrid foam for infrared stealth, thermal insulation, and microwave absorption. ACS Appl Mater Interfaces 12:28727-28737. https://doi.org/10.1021/acsami.0c09202

Gunasekara DSW, He Y, Fang S, Zhao LD, Liu H, Liu L (2020) High-repeatability macro-porous sponge piezoresistive pressure sensor with dopamine/polypyrrole composite coating based on in situ polymerization method. Appl Phys A 126:789. https://doi.org/ 10.1007/s00339-020-03962-z

Haque MM, Wong DKY (2017) Improved dye entrapment-liberation performance at electrochemically synthesized polypyrrole-reduced graphene oxide nanocomposite films. J Appl Electro-chem 47:777-788. https://doi.org/10.1007/s10800-017-1079-9

Humpolíček P, Kašpárková V, Pecherník J, Stejskal J, Bober P, Capák-ová Z, Radaskiewicz KA, Junkar I, Lehocký M (2018) The biocompatibility of polyaniline and polypyrrole: a comparative study of their cytotoxicity, embryotoxicity and impurity profile. Mater Sci Eng C 91:303-310. https://doi.org/10.1016/).msec. 2018.05.037

Ivanova VT, Garina EO, Burtseva EI, Kirillova ES, Ivanova MV, Stejskal J, Sapurina IYu (2017) Conducting polymers as sorbents of influenza viruses. Chem Pap 71:495-503. https://doi.org/10. 1007/s 11696-016-0068-5

Janaki V, Vijayaraghavan K, Oh BT, Ramasamy AK, Kamala-Kannan S (2013) Synthesis, characterization and application of cellulose/ polyaniline nanocomposite for the treatment of simulated textile effluent. Cellulose 20:1153-1166. https://doi.org/10.1007/ s10570-013-9910-x

Jing XX, Zhou L, Kang WJ, Wang L, Wei DH, Qu KG, Li R, Chen BL, Guo ZJ, Li HB (2020) Regulating capacitative performance of monolithic carbon sponges by balancing heteroatom content, surface area and graphitization degree. ChemNanoMat 6:15071512. https ://doi.org/10.1002/cnma.2020003 58

Jorio A, Dresselhaus M, Saito R, Dresselhaus GF (2011) Raman spectroscopy in graphene related systems. Wiley-VCH Verlag, Weinheim

Kadlec K, Kminek M, Kadlec P (2019) Measurement and control of chemical, food, and biotechnological processes. Key Publishing, London, England

Kazantseva NE, Vilčáková J, Křesálek V, Sáha P, Sapurina I, Stejskal J (2004) Magnetic behaviour of composites containing polyaniline-coated manganese-zinc ferrite. J Magn Magn Mater 269:3037. https://doi.org/10.1016/S0304-8853(03)00557-2

Kopecká J, Kopecký D, Vrňata M, Fitl P, Stejskal J, Trchová M, Bober P, Morávková Z, Prokeš J, Sapurina I (2014) Polypyrrole nanotubes: mechanism of formation. RSC Adv 4:1551-1558. https:// doi.org/10.1039/c3ra45841e

Lavrador P, Esteves MR, Gaspar VM, Mano JF (2021) Stimuli-respon-sive nanocomposite hydrogels for biomedical applications. Adv Funct Mater 31:2005941. https://doi.org/10.1002/adfm.20200 5941

Li CW, Jiang DG, Huo BB, Ding MC, Huang CC, Jia DD, Li HX, Liu CY, Liu JQ (2019) Scalable and robust bilayer polymer foams for highly efficient and stable solar desalination. Nano Energy 60:841-849. https://doi.org/10.1016/j.nanoen.2019.03.087

Li YJ, Li WY, Kick C, Zhao XM, Wu HY (2020a) Preparation of polypyrrole/polyurethane foam composite material. Fibre Text Eastern Eur 28:69-73. https://doi.org/10.5604/01.3001.0013. 9022

Li Y, Wang YP, Bian C, Stejskal J, Zheng YS, Jing XL (2020b) Azo dye aggregates and their role in the morphology and conductivity of polypyrrole. Dye Pigment 177:108329. https://doi.org/10. 1016/j. dyepig .2020.108329

Li Y, Wang YP, Liu XQ, Wang S, Jing XL (2021) Facilely prepared conductive hydrogels based on polypyrrole nanotubes. Chem Pap 75: early view. https://doi.org/10.1007/s11696-021-01559-1

Lin J, Xu YL, Wang J, Zhang BF, Li D, Wang C, Jin YL, Zhu JB (2018) Nitrogen-doped hierarchically porous carbonaceous nanotubes for lithium ion batteries. Chem Eng J 352:964-971. https://doi. org/10.1016/j.cej.2018.06.057

Liu Q, Meng K, Ding K, Wang YB (2015) A superhydrophobic sponge with hierarchical structure as an efficient and recyclable oil absorbent. ChemPlusChem 80:1435-1439. https://doi.org/10. 1002/cplu.201500109

Liu QF, Zang LM, Qiao X, Qiu JH, Wang X, Hu L, Yang J, Yang C (2019) Compressible all-in-one supercapacitor with adjustable output voltage based on polypyrrole-coated melamine foam. Adv Electron Mater 5:1900724. https://doi.org/10.1002/201900724

Liu ML, Li L, Sun YX, Fu ZJ, Cao XL, Sun SP (2020) Scalable conductive polymer membranes for ultrafast organic pollutants removal. J Membr Sci 617:118644. https://doi.org/10.1016/j. memsci.2020.118644

Lu Y, Biswas MC, Guo Z, Jeon JW, Wujcik EK (2019) Recent developments in bio-monitoring via advanced polymer nanocomposite-based wearable strain sensors. Biosens Bioelectron 123:167-177. https://doi.org/10.1016/j.bios.2018.08.037

Mahlangu T, Das R, Abia LK, Onyango M, Ray SS, Maity A (2019) Thiol-modified magnetic polypyrrole nanocomposite: an effective adsorbent for the adsorption of silver ions from aqueous solution and subsequent water disinfection by silver-laden nanocomposite. Chem Eng J 360:423-434. https://doi.org/10.1016/j. cej.2018.11.231

Maldonado-Larios L, Mayen-Mondragón R, Martinez-Orozco RD, Páramo-García U, Gallardo-Rivas MV, Garcia-Alamilla R (2020) Electrochemically-assisted fabrication of titanium-dioxide/poly-aniline nanocomposite films for the electroremediation of congo red in aqueous effluents. Synth Met 268:116464. https://doi.org/ 10.1016/j. synthmet.2020.116464

Maráková N, Humpoliček P, Kašpárková V, Capáková Z, Martinková L, Bober P, Trchová M, Stejskal J (2017) Antimicrobial activity and cytotoxicity of cotton fabric coated with conducting polymers, polyaniline or polypyrrole, and with deposited silver nanoparticles. Appl Surf Sci 396:169-176. https://doi.org/10.1016/j. apsusc.2016.11.024

Mashkoor F, Nazar A (2020) Facile synthesis of polypyrrole decorated chitosan-based magadsorbent: characterization, performance, and applications in removing cationic and anionic dyes from aqueous medium. Int J Biol Macromol 161:88-100. https://doi. org/10.1016/j.ijbiomac.2020.06.015

Milakin KA, Acharya U, Trchová M, Zasońska BA, Stejskal J (2020) Polypyrrole/gelatin cryogel as a precursor for a macroporous conducting polymer. React Funct Polym 157:104751. https:// doi.org/10.1016/j .reactfunctpoly m. 2020.104751

Minisy IM, Acharya U, Kobera L, Trchová M, Unterweger C, Bre-itenbach S, Brus J, Pfleger J, Stejskal J, Bober P (2020a) Highly conducting 1-D polypyrrole prepared in the presence of safranin. J Mater Chem C 8:12140-12147. https://doi.org/10.1039/d0tc0 2838j

Minisy IM, Zasońska B, Petrovský E, Veverka P, Šeděnková I, Hromádková J, Bober P (2020b) Poly(p-phenylenediamine)/ maghemite composite as a highly effective adsorbent for anionic dye removal. React Funct Polym 146:104436. https://doi.org/10. 1016/j.reactfunctpolym.2019.104436

Moučka R, Sedlačík M, Prokeš J, Kasparyan H, Valtera S, Kopecký D (2020) Electromagnetic interference shielding of polypyrrole nanostructures. Synth Met 269:116572. https://doi.org/10.1016/]'. synthmet.2020.116573

Moučka R, Sedlačik M, Kasparyan H, Prokeš J, Trchová M, Has-souna F, Kopecký D (2021) One-dimensional nanostructures of polypyrrole for shielding of electromagnetic interference in the microwave region. Int J Mol Sci 21:8814. https://doi.org/10. 3390/ijms21228814

$\ddot{O}zt\ddot{u}$rk A, Yurtcan AB (2018) Synthesis of polypyrrole (PPy) based porous N-doped carbon nanotubes (N-CNTs) as catalyst support for PEM fuel cells. Int J Hydrogen Energy 43:18595-18571. https://doi.org/10.1016/j.ijhydene.2018.05.106

Peng CW, Yu J, Chen SH, Wang L (2019) High performance supercapacitor based on ultralight and elastic three-dimensional carbon foam/reduced graphene/polyaniline nanocomposites. Chin Chem Lett 30:1127-1140. https://doi.org/10.1016/j.cclet.2019.02.007

Pérez-Rodríguez P, Ovando-Medina VM, Martinez-Amador SY, Rodriguez-de la Garza JA (2016) Bioanode in polyurethane/ graphite/polypyrrole composite in microbial fuel cells. Bio-technol Bioprocess Eng 21:305-313. https://doi.org/10.1007/ s12257-015-0628-5

Petcharoen K, Sirivit A (2012) Synthesis and characterization of magnetite particles via the chemical co-precipitation method. Mater Sci Eng B 177:421-427. https://doi.org/10.1016/]'.mseb.2012. 01.003

Pethsangave DA, Khose RV, Wadekar PH, Kulal DK, Some S (2020) One-pot synthetic approach for magnetically separable graphene nanocomposite for dye degradation. ChemistrySelect 5:15161525. https://doi.org/10.1002/slct.201903966

Pimenta MA, Dresselhaus G, Dresselhaus MS, Canęado LG, Jorio A, Saito R (2007) Studying disorder in graphite-based systems by Raman spectroscopy. Phys Chem Chem Phys 20:1276-1291. https://doi.org/10.1039/b613962k

Qi L, Gong JC (2020) Facile in-situ polymerization of polyaniline-functionalized melamine sponge preparation for mass spectro-metric monitoring of perfluorooctanoic acid and perfluorooctane sulfonate from biological samples. J Chromatogr A 1616:460777. https://doi.org/10.1016/jhchroma.2019.460777

Qiu GH, Wang Q, Nie M (2006) Polypyrrole-Fe3O4 magnetic nanocomposite prepared by ultrasonic irradiation. Macromol Mater Eng 291:68-74. https://doi.org/10.1002/mame.299500285

Raj BGS, Ko TH, Acharya J, Seo MK, Khil MS, Kim HY, Kim BS (2020) A novel Fe2O3-decorated N-doped CNT porous composites derived from tubular polypyrrole with excellent rate capability and cycle stability as advanced supercapacitor anode materials. Electrochim Acta 334:135627. https://doi.org/10.1016Zj.elect acta.2020.135627

Riede A, Helmstedt M, Sapurina I, Stejskal J (2002) In situ polymerized polyaniline films 4. Film formation in dispersion polymerization of aniline. J Colloid Interface Sci 248:413-418. https:// doi.org/10.1006/jcis.2001.8197

Ruan CP, Ai KL, Li XB, Lu LH (2014) A superhydrophobic sponge with excellent absorbency and flame retardancy. Angew Chem Int Ed 53:5556-5560. https://doi.org/10.1002/anie.201400775

Ruan BY, Guo HP, Liu QN, Shi DQ, Chou SL, Liu HK, Chen GH, Qang JZ (2016) 3-D structured SnO2-polypyrrole nanotubes applied in Na-ion batteries. RSC Adv 6:103124-103131. https:// doi.org/10.1039/c6ra21139a

Sapurina I, Stejskal J, Šeděnková I, Trchová M, Kovářová J, Hromád-ková J, Kopecká J, Cieslar M, Abu El-Nasr A, Ayad MM (2016) Catalytic activity of polypyrrole nanotubes decorated with noble-metal nanoparticles and their conversion to carbonized analogues. Synth Met 214:14-22. https://doi.org/10.1016/)'.synth met.2016.01.009

Sapurina IYu, Shishov MA, Ivanova VT (2020) Sorbents for water purification based on conjugated polymers. Russ Chem Rev 89:1115-1131. https://doi.org/10.1070/RCR4955

Shi PF, Wang C, Sun JY, Lin P, Xu XT, Yang T (2020) Thermal conversion of polypyrrole nanotubes to nitrogen-doped carbon nanotubes for efficient water desalination using membrane capacitive deionization. Separ Purif Technol 235:116196. https://doi.org/10. 1016/j.seppur.2019.116196

Sparavigna AM, Florio L, Avloni J, Henn A (2010) Polypyrrole coated PET fabrics for thermal applications. Mater Sci Appl 1:253-259. https://doi.org/10.4236/msa.2010.14037

Stejskal J (2013) Conducting polymer-silver composites. Chem Pap 67:814-848. https://doi.org/10.2478/s11696-012-0304-6

Stejskal J (2015) Polymers of phenylenediamines. Prog Polym Sci 41:1-31. https://doi.org/10.1016/j.progpolymsci.2014.10.007

Stejskal J (2017) Conducting polymer hydrogels. Chem Pap 71:269291. https ://doi.org/10.1007/s 11696-016-0072-9

Stejskal J, Trchová M (2018) Conducting polypyrrole nanotubes. Chem Pap 72:1563-1595. https://doi.org/10.1007/s11696-018-0394x

Stejskal J (2020a) Interaction of conducting polymers, polyaniline and polypyrrole, with organic dyes: polymer morphology control, dye adsorption and photocatalytic decomposition. Chem Pap 74:1-54. https://doi.org/10.1007/s11696-019-00982-9

Stejskal J (2020b) Conducting polymers are not just conducting: a perspective for emerging technology. Polym Int 69:662-664. https:// doi.org/10.1002/pi.5947

Stejskal J, Trchová M, Sapurina I (2005) Flame-retardant effect of polyaniline coating deposited on cellulose fibers. J Appl Polym Sci 98:2347-2354. https://doi.org/10.1002/app.22144

Stejskal J, Prokeš J, Trchová M (2008) Reprotonation of polyaniline: a route to various conducting polymer materials. React Funct Polym 68:1355-1361. https://doi.org/10.1016/j.reactfunctpolym. 2008.06.012

Stejskal J, Bogomolova OE, Blinova NV, Trchová M, Šeděnková I, Prokeš J, Sapurina I (2009) Mixed electron and proton conductivity of polyaniline films in aqueous solutions of acids: beyond the 1000 S cm-1 limit. Polym Int 58:872-879. https://doi.org/ 10.1002/pi.2605

Stejskal J, Trchová M, Bober P, Morávková Z, Kopecký D, Vrňata M, Prokeš J, Varga M, Watzlová E (2016) Polypyrrole salts and bases: superior conductivity of nanotubes and their stability towards the loss of conductivity by deprotonation. RSC Adv 6:88382. https ://doi.org/10.1039/c6ra19461 c

Stejskal J, Prokeš J (2020) Conductivity and morphology of polyaniline and polypyrrole prepared in the presence of organic dyes. Synth Met 264:116373. https://doi.org/10.1016/j.synthmet.2020. 116373

Stejskal J, Trchová M, Kasparyan H, Kopecký D, Kolská Z, Prokeš J, Křivka I, Vajďák J, Humpolíček P (2021a) Pressure-sensitive conducting and antibacterial materials obtained by in-situ dispersion coating of macroporous melamine sponges with polypyrrole. ACS Omega 6: early view. https://doi.org/10.1021/acsom ega.1c02330

Stejskal J, Kohl M, Trchová M, Kolská Z, Pekárek M, Křivka I, Prokeš J (2021b) Conversion of conducting polypyrrole nanostructures to nitrogen-containing carbons and its impact on the adsorption of organic dye. Mater Adv 2:706-717. https://doi.org/10.1039/ d0ma00730g

Stejskal J, Sapurina I, Vilčáková J, Jurča M, Trchová M, Kolská Z, Prokeš J, Křivka I (2021c) One-pot preparation of conducting melamine/polypyrrole/magnetite ferrosponge. ACS Appl Polym Mater 3:1107-1115. https://doi.org/10.1021/acsapm.0c01331

Stejskal J, Kopecký D, Kasparyan H, Vilčáková J, Prokeš J, Křivka I (2021d) Melamine sponges decorated with polypyrrole nanotubes as macroporous conducting pressure sensors. ACS Appl Nano Mater 4: early view. https://doi.org/10.1021/acsapm.0c016 34

Sun YY, Jia DD, Zhang AT, Tian JM, Zheng YW, Zhao W, Cui L, Liu JQ (2019) Synthesis of polypyrrole coated melamine foam by in-situ interfacial polymerization method for highly compressible and flexible supercapacitor. J Colloid Interface Sci 557:617-627. https://doi.org/10.1016/j.jcis.2019.09.065

Tomczykowa M, Polonska-Brzezinska ME (2019) Conducting polymers, hydrogels, and their composites: preparation, properties and bioapplications. Polymers 11:350. https://doi.org/10.3390/ 11020350

Trchová M, Stejskal J (2018) Resonance Raman spectroscopy of conducting polypyrrole nanotubes: disordered surface versus ordered body. J Phys Chem A 122:9298-9306. https://doi.org/10.1021/ acs.jpca.8b09794

Vali SA, Baghdadi M, Abdoli MA (2018) Immobilization of polyaniline nanoparticles on the polyurethane foam derived from waste materials: a porous reactive fixed-bed medium for removal of mercury from contaminated waters. J Environ Chem Eng 6:6612-6622. https://doi.org/10.1016/j.jece.2018.09.042

Varsheny S, Dhawan SK (2017) Designing of materials for EMI shielding applications. In: Sebastian MT, Ubic R, Jantunen H (eds) Microwave materials and applications, Vol 2, Chap 13. Wiley, UK

Wan YQ, Qin N, Wang YF, Zhao QB, Wang Q, Yuan PC, Wen Q, Wei H, Zhang XY, Ma N (2020) Sugar-templated conductive polyurethane-polypyrrole sponges for wide-range force sensing. Chem Eng J 383:123103. https://doi.org/10.1016/j.cej.2019.123103

Wang LC, Zhang CG, Jiao X, Yuan ZH (2019) Polypyrrole-based hybrid nanostructures grown on textile for wearable supercapacitors. Nano Res 12:1129-1137. https://doi.org/10.1007/ s 12274-019-2360-5

Wei CZ, Xu Q, Chen ZQ, Rao WD, Fan LL, Yuan Y, Bai ZK, Xu J (2017) An all-solid-state yarn supercapacitor using cotton yarn electrodes coated with polypyrrole nanotubes. Carbohydr Polym 169:50-57. https://doi.org/10.1016/j.carbpol.2017.04.002

Wu MC, Zhao TS, Zhang RH, Wei L, Jiang HR (2018) Carbonized tubular polypyrrole with a high activity for the Br2/Br- redox reaction in zinc-bromine flow batteries. Electrochim Acta 284:569-576. https://doi.org/10.1016/j.electacta.2018.07.192

Wu XW, Lei YG, LiSH, Huang JY, Teng L, Chen Z, Lai YK (2021) Photothermal and Joule heating-assisted thermal management sponge for efficient cleanup of highly viscous crude oil. J Hazard Mater 403:124090. https://doi.org/10.1016/j.jhazmat.2020. 124090

Xie J, Pan W, Chen Y, Guo Z (2020) Preparation of polypyrrole coated on polyester cleanroom wiper as heater device. J Eng Fiber Fabric 15:1-7. https://doi.org/10.1177/1558925020925408

Xu HT, Wu JS, Qi LJ, Chen Y, Wen Q, Duan TG, Wang YY (2018) Preparation and microbial fuel cell application of sponge-structured hierarchical polyaniline-texture bioanode with an integration of electricity generation and energy storage. J Appl Electro-chem 48:1285-1295. https://doi.org/10.1007/s10800-018-1252-9

Xu Y, Ma JX, Han Y, Xu HB, Wang Y, Qi DP, Wang W (2020) A simple and universal strategy to deposit Ag/polypyrrole on various substrates for enhanced interfacial solar evaporation and antibacterial activity. Chem Eng J 384:123379. https://doi.org/10. 1016/j.cej.2019.123379

Xu LL, Yang Y, Mao XK, Li Z (2021) Self-powerbility in electrical stimulation drug delivery system. Adv Mater Techol 6:202100055. https://doi.org/10.1002/admt.202100055

Yan XR, Hu MJ, Liu JX, Yan L, Zhang NB, Gao JF, Liu JZ, Shan GC, Yang J (2020) Compressible metalized soft magnetic sponges with tailorable electrical and magnetic properties. ChemNano-Mat 6:316-325. https://doi.org/10.1002/cnma.201900646

Ye XL, Chen CF, Ai SF, Hou B, Zhang JX, Liang XH, Zhou QB, Liu HZ, Cui S (2019) Synthesis and microwave properties of novel reticulation SiC/porous melamine-derived carbon foam. J Alloy Comp 791:883-891. https://doi.org/10.1016/j.jallcom. 2019.03.384

Zare EN, Makvandi P, Ashtan B, Rossi F, Motahari A, Perale G (2020) Progress in conductive polyaniline-based nanocomposites for biomedical applications: a review. J Med Chem 63:1-22

Zhang M, Wang CY, Ma YH, Du XL, Shi YH, Li J, Shi JY (2020) Fabrication of superwetting, antimicrobial and conductive fibrous membranes for removing/collecting oil contaminants. RSC Adv 10:21636-21642. https://doi.org/10.1039/d0ra02704a